



OPEN ACCESS

EDITED BY

James Tee,
University of Canterbury, New Zealand

REVIEWED BY

Fuat Balci,
University of Manitoba, Canada
Peter Shizgal,
Concordia University, Canada
Hessameddin Akhlaghpour,
The Rockefeller University,
United States

*CORRESPONDENCE

Germund Hesslow
randy.gallistel@gmail.com

RECEIVED 15 August 2022

ACCEPTED 21 September 2022

PUBLISHED 03 November 2022

CITATION

Gallistel CR, Johansson F,
Jirenhd D-A, Rasmussen A, Ricci M
and Hesslow G (2022) Quantitative
properties of the creation
and activation of a cell-intrinsic
duration-encoding engram.
Front. Comput. Neurosci. 16:1019812.
doi: 10.3389/fncom.2022.1019812

COPYRIGHT

© 2022 Gallistel, Johansson, Jirenhd,
Rasmussen, Ricci and Hesslow. This is
an open-access article distributed
under the terms of the [Creative
Commons Attribution License \(CC BY\)](#).
The use, distribution or reproduction in
other forums is permitted, provided
the original author(s) and the copyright
owner(s) are credited and that the
original publication in this journal is
cited, in accordance with accepted
academic practice. No use, distribution
or reproduction is permitted which
does not comply with these terms.

Quantitative properties of the creation and activation of a cell-intrinsic duration-encoding engram

Charles Randy Gallistel¹, Fredrik Johansson²,
Dan-Anders Jirenhd², Anders Rasmussen², Matthew Ricci³
and Germund Hesslow^{2*}

¹Rutgers Center for Cognitive Science, Piscataway, NJ, United States, ²Department of Experimental Medical Science, Faculty of Medicine, Lund University, Lund, Sweden, ³Carney Institute for Brain Sciences, Brown University, Providence, RI, United States

The engram encoding the interval between the conditional stimulus (CS) and the unconditional stimulus (US) in eyeblink conditioning resides within a small population of cerebellar Purkinje cells. CSs activate this engram to produce a pause in the spontaneous firing rate of the cell, which times the CS-conditional blink. We developed a Bayesian algorithm that finds pause onsets and offsets in the records from individual CS-alone trials. We find that the pause consists of a single unusually long interspike interval. Its onset and offset latencies and their trial-to-trial variability are proportional to the CS-US interval. The coefficient of variation ($CoV = \sigma/\mu$) are comparable to the CoVs for the conditional eye blink. The average trial-to-trial correlation between the onset latencies and the offset latencies is close to 0, implying that the onsets and offsets are mediated by two stochastically independent readings of the engram. The onset of the pause is step-like; there is no decline in firing rate between the onset of the CS and the onset of the pause. A single presynaptic spike volley suffices to trigger the reading of the engram; and the pause parameters are unaffected by subsequent volleys. The Fano factors for trial-to-trial variations in the distribution of interspike intervals within the intertrial intervals indicate pronounced non-stationarity in the endogenous spontaneous spiking rate, on which the CS-triggered firing pause supervenes. These properties of the spontaneous firing and of the engram read out may prove useful in finding the cell-intrinsic, molecular-level structure that encodes the CS-US interval.

KEYWORDS

Shannon information, timing, cerebellum, classical conditioning, Purkinje cell, reinforcement learning

Introduction

The neurobiological memory mechanism carries forward in time, in computationally accessible form, abstract facts gleaned from experience, such as the duration of experienced intervals (Savastano and Miller, 1998; Balsam et al., 2010; Buonomano, 2017; Mattell and Della Valle, 2018). The experimental literature on the neurobiology of memory is vast, but little of it focuses on how and where specified information is encoded in specified neurons, where information is to be understood in Shannon's sense. Only in Shannon's sense is information a measurable physical quantity, which is what one needs if one is looking for a neurobiological structure that encodes information.

The cerebellar Purkinje cell is the location of a memory for a quantitative experiential fact, namely, the duration of the inter-stimulus interval in the classically conditioned eye blink (Jirenhed et al., 2007, 2017; Johansson et al., 2014, 2015). The behaviorally observed conditional blink is driven by a conditional pause response in the spontaneous firing of specific blink-controlling Purkinje cells. These cells are inhibitory on the cerebellar nuclei, so a pause in Purkinje cell firing translates into an excitatory output signal from the cerebellum. The conditional firing pause is the only cellular level associative learning phenomenon whose quantitative properties align with the behaviorally established properties of associative learning (Gallistel and Matzel, 2013; Jirenhed and Hesslow, 2016).

In a Pavlovian delay conditioning protocol, a neutral stimulus (the conditional stimulus or CS for short) is repeatedly presented at a short, fixed latency prior to an unconditional stimulus (US for short), which is a stimulus that directly elicits a reflexive response in the naive subject. In an eye blink conditioning protocol, the US is a threat to the eye. The CS is any of a wide variety of stimuli that do not elicit a blink prior to conditioning. When the US follows the CS over a number of trials at intervals in the range from 0.1 to as much as 2.0s, a conditional blink to the CS develops. The number of conditioning trials prior to its appearance varies from a few to several hundred, depending on the subject and the parameters of the protocol (Gallistel and Gibbon, 2000; Gallistel et al., 2004).

The conditional blink to the CS commences prior to the onset of the US, and it occurs on probe trials, when there is no US. The latency at which the CS evokes the blink varies in proportion to the interval that elapses between CS onset and US onset, so that the closure of the lid or membrane peaks near the moment when the threat to the eye is anticipated (White et al., 2000; Kehoe et al., 2009). Thus, this simple Pavlovian conditioning procedure inscribes in the brain a simple quantitative fact—the duration of the CS-US interval. The inscribed quantitative fact is read out into an appropriately timed behavior whenever the CS is again presented. The locus of the material change in the brain that encodes this fact is a prime target in the search for the engram, the neurobiological basis of memory.

The CS-conditional blink of the eye has been obtained in decerebrate preparations of cats, rabbits, ferrets and guinea pigs (Norman et al., 1977; Mauk and Thompson, 1987; Kelly et al., 1990; Hesslow and Ivarsson, 1994; Kotani et al., 2002), proving that the forebrain is not essential; the brain stem alone is sufficient. Within the brain stem, the cerebellum is known to be the main locus of the memory trace (McCormick and Thompson, 1984; Yeo, 1991; Krupa et al., 1993; Hesslow and Yeo, 2002; Thompson and Steinmetz, 2009; Freeman, 2015). Disruption of cerebellar afferent signaling by a cerebral-vascular accident prevented eye blink conditioning in a human subject (Solomon et al., 1989).

The cerebellar Purkinje cell is among the largest neurons in the vertebrate brain (Knierem, 1997; Llinas et al., 2004; Apps and Garwicz, 2005). It is the sole output of the cerebellar cortex. Its immense, flat, densely arborized dendritic tree straddles a subset of the dense projections of parallel fibers. The parallel fibers arise from the tiny granule cells in the granular layer of the cerebellar cortex. They project upward to the top layer of the cerebellar cortex, where they bifurcate and run parallel to the folds of the cerebellar cortex. They pass through and make glutamatergic synapses on the staggered dendritic trees of numerous Purkinje cells. On the order of 200,000 parallel fibers synapse on the dendrites of each Purkinje cell. The granule cells from which they arise constitute substantially more than 50% of the neurons in a vertebrate brain (D'Angelo et al., 2013).

Climbing fibers provide the only other excitatory input to Purkinje cells (Knierem, 1997; Llinas et al., 2004; Apps and Garwicz, 2005). They arise from cells in the inferior olivary nucleus. In stark contrast to the parallel fibers, only one climbing fiber innervates a Purkinje cell. Its terminal arbor wraps the cell with a dense engulfing bush of synapses. Short bursts of high-frequency presynaptic spikes in the climbing fiber produce the complex, multi-modal post-synaptic spike, which is thought to control Purkinje cell spiking rates and induce learning.

The main site of learning in the decerebrate preparation is the cerebellar cortex (Yeo et al., 1984, 1985a,b, 1986; Hesslow, 1994a,b; Heiney et al., 2014; Johansson et al., 2016; Ten Brinke et al., 2017), which consists of roughly 1,000 microzones (Apps and Garwicz, 2005). Each part of the body maps by way of the climbing fiber system to several disparately located microzones. The Purkinje cells whose conditional pauses we here analyze are located in the C3 zone of the ferret cerebellum, the area that has been shown to mediate the classically conditioned eye blink (Yeo et al., 1985a,b, 1986; Hesslow, 1994a,b; Heiney et al., 2014; Jirenhed and Hesslow, 2016). Like most Purkinje cells, these have a high spontaneous firing rate—on the order of 40–80 Hz.

The conditional pause in Purkinje cell firing develops in the decerebrate ferret even when the CS is direct electrical stimulation of the parallel fibers and the US is direct electrical stimulation of the climbing fiber (Johansson et al., 2014). Stimulation of off-beam parallel fibers—fibers that do not synapse on the Purkinje cell from which one is

recording—produces a profound inhibition of the spontaneous firing, presumably by way of the stellate cells or the basket cells or both. However, a dose of a GABA blocker sufficient to block this inhibitory effect does not block the elicitation of the conditional pause (Johansson et al., 2014). This result implies that the pause is not mediated by input from the inhibitory interneurons synapsing on the Purkinje cell. This conclusion is further strengthened by the fact that the ability of the glutamatergic input from the parallel fibers to trigger the pause in firing is blocked by the infusion of an agent that selectively blocks the mGlu7 receptor in the synapse that a parallel fiber makes onto a Purkinje cell (Johansson, 2015; Johansson et al., 2015). Together these results make a strong case that the mechanism that times the CS-US interval, the mechanism that records into memory the result of that timing (the duration of the interval) and the mechanism that reads the remembered durations out into a pause of corresponding duration are intrinsic to the Purkinje cell itself (Johansson, 2019).

Previous analyses of the Purkinje cell pause responses have been based on averaging across trials, such as peristimulus time histograms. Although an indispensable technique, averaging can conceal and distort important features of the individual responses. For instance, sudden response onsets with variable latencies will look like gradual onsets. We have therefore re-analyzed a large body of data and here report the trial-by-trial statistics of the conditional pauses obtained from decerebrate ferrets under three experimental conditions (Figure 1). In the first conditions, the CS was pulsatile electrical stimulation of the mossy fibers at 50 Hz (The mossy fibers are the input to the granule cells.) The US was two short bursts of pulsatile electrical stimulation to the inferior olive or to a climbing fiber. In the second, the CS was pulsatile electrical stimulation of the dorsum of the forepaw at 50 Hz and the US was two short bursts of pulsatile electrical stimulation to a climbing fiber.

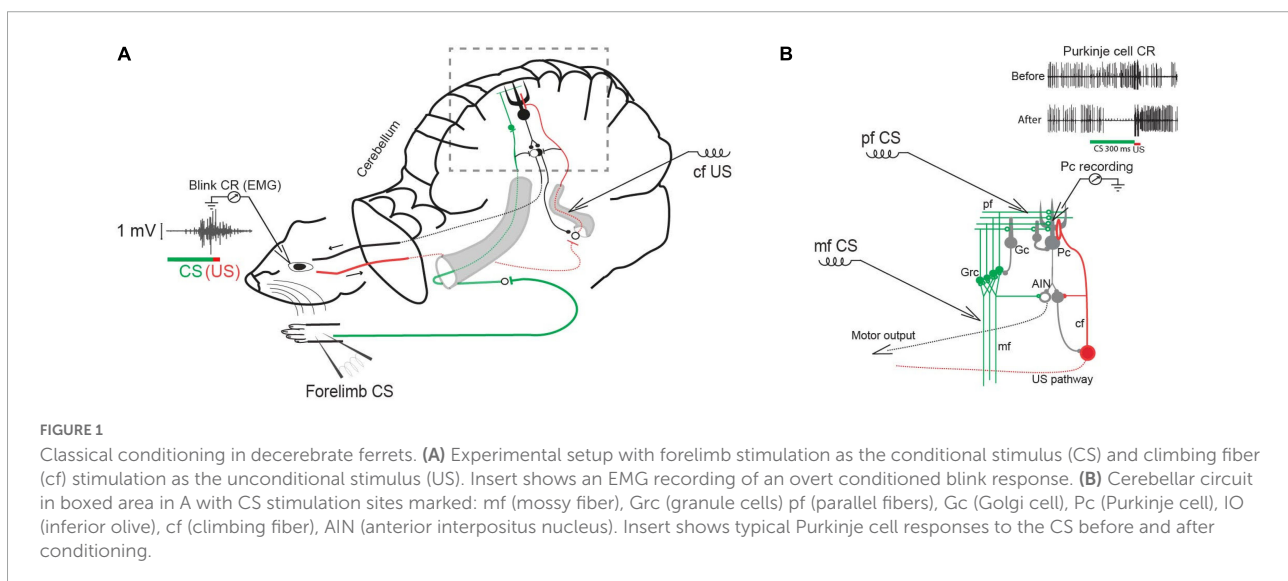
In the third, the CS was pulsatile electrical stimulation of the parallel fibers, which are the immediate presynaptic input to the Purkinje cell; the US was again two short bursts of pulsatile electrical stimulation to a climbing fiber. The CS-US interval used in training varied from 0.15 to 0.45s. The CS stimulation terminated just before US onset in some cases, while in others, it continued well beyond US offset.

Determining trial-by-trial pause statistics

The conditional pause is commonly visualized by a raster plot of a sequence of probe (that is, CS alone) trials (Figure 2A). Its average duration may be estimated from the peri-CS histogram of spike counts (Figure 2B). In this work, we determine the distribution of pause statistics for individual trials—onset latencies, offset latencies, pause widths, pause depths and the abruptness of pause onsets. In the Discussion, we consider how these statistics constrain possible mechanisms for the generation of the pauses.

The compilation of trial-by-trial pause statistics presupposes an algorithm for determining their onsets and offsets. We developed a Bayesian algorithm that uses the statistics from the peri-stimulus histogram to set prior probabilities on the locations of the onsets and offsets on individual trials and on the rates of firing before, during, and after the pause. The data and the Matlab™ code implementing our analyses are in a publicly accessible repository.¹ The algorithm delivered trial-by-trial estimates of pause onset, pause offset, the weights of the evidence for the onset and for the offset. It also delivered

¹ <https://github.com/CRGallistel/QuantPropPrkjPauseGH>



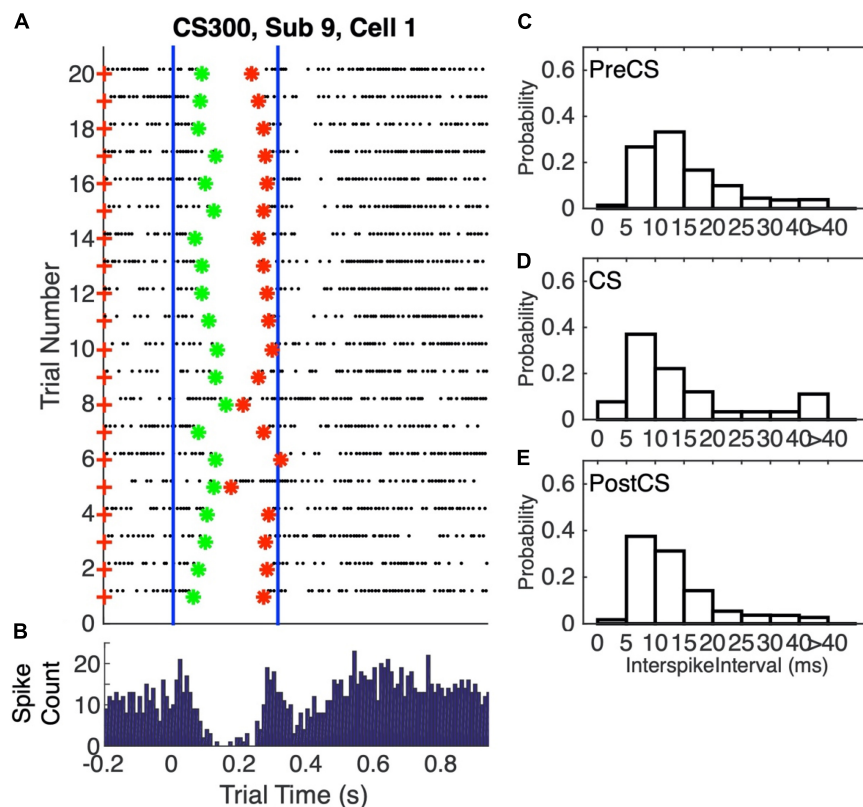


FIGURE 2

(A) Spike raster plot of 20 successive probe trials (trials without a US) following conditioning with a 0.3 s CS-US interval. The CS was 0.3 s stimulation of the dorsum of the forepaw at 50 Hz, both during training, when US onset immediately followed CS termination, and in these probe trials. The US during training was two 5-pulse bursts of 500 Hz stimulation of the climbing fiber input (5 ms between the bursts). The blue vertical lines mark the beginning and end of the CS-US interval. Green asterisks mark the pause onsets, as determined by our algorithm for estimating pause onsets and offsets; red asterisks mark the estimated pause offsets. (B) Peri-CS histogram, counting spikes across the 20 trials into successive 10 ms wide bins. (C–E) Probability distribution functions (normalized histograms, with 5 ms wide bins) on the inter-spike intervals during the 0.3 s preceding the CS (C), during the CS-US interval (D), and during the 1 s after the CS (E).

the duration of the longest inter-spike interval between these estimates, which may be considered an estimate of the depth of a pause. It also delivered the latency from pause onset to the onset of the longest inter-spike interval. This may be considered a measure of the abruptness of pause onset. Finally, it delivered the interval from the estimate of pause onset to the estimate of pause offset, which is an estimate of the width of the pause.

Experiment 1: Acquisition of the conditional pause

Recordings were made from ten Purkinje cells in the eyeblink-controlling microzone within the C3 zone of the ferret cerebellar cortex during a conditioning protocol in which the CS was stimulation of the mossy fibers at 50 Hz. The US was direct stimulation of the inferior olive ($n = 5$) or climbing fibers ($n = 5$) with two short bursts of 5 pulses each, delivered at 500 Hz,

with an interval between the bursts of 12 ms (first 7 subjects) or 4 ms (last 3 subjects). The ferrets were decerebrated before the experiment began.

In this and all subsequent experiments, each Purkinje cell was identified as an eyeblink cell by the presence of microzone-defining short-latency (10–12 ms) complex spike responses to brief electrical stimulation of the periocular receptive field (Hesslow, 1994b).

In Cells/Subjects 1 through 7, CS stimulations terminated after 0.3 s, and the US onset occurred 0.2 s later. In the last three Cells/Subjects, US onset occurred 0.2 s after CS onset and the CS stimulation continued through and beyond US onset and offset. This was done to deconfound the effects of US onset from those of CS offset.

Recordings were initiated in the naive state, i.e., before the animal had been exposed to any (or only a few) paired stimulus presentations and continued for up to 4 h, until a conditional pause was apparent over a sequence of trials. The inter-trial interval (the interval between CS onsets) was 15 s.

Results of the analysis

Complex and variable course of conditioning

Figure 3 shows two raster plots with complete trial sequences. They are chosen to illustrate the complexity and diversity of what is seen during the training period, when the conditional pause develops.

In the left panel, one sees vertical lines of spikes at 20 ms intervals during the CS. These are clearly driven by the input, which was pulsatile mossy-fiber stimulation at 50 Hz. Early in training, the overall frequency of spikes is greater during the CS than before its onset. After about Trial 50, there are hints of a fall in frequency about half way through the CS, but this fall is more than offset by a clear increase in firing frequency in the first 100 ms. After 250 trials, a pause is evident, and the spikes elicited by the stimulation pulses begin to be suppressed during this pause. After 600 trials, this suppression is almost complete.

In the right panel, there is no evidence of spikes elicited by the stimulation pulses. The pause is evident from the beginning, but it becomes more pronounced after about 180 trials.

The responses to the two brief bursts of US stimulation of the climbing fiber differ markedly between the two panels, and these responses to the US evolve in complex and disparate ways over the course of training. In some records, pronounced variations in firing rate are seen for several hundred milliseconds after US stimulation. These complexly evolving post-US variations in firing differ markedly from cell to cell. We do not attempt to analyze them in the present work.

Non-stationarity in basal firing rate

There is substantial trial-to-trial variability in the firing rate prior to CS onset. Computation of the Fano factors for the spike count in the 1 s window immediately preceding CS onset shows that this variability is not consistent with a stationary Poisson process. If it were, the Fano factor, which is the ratio of the

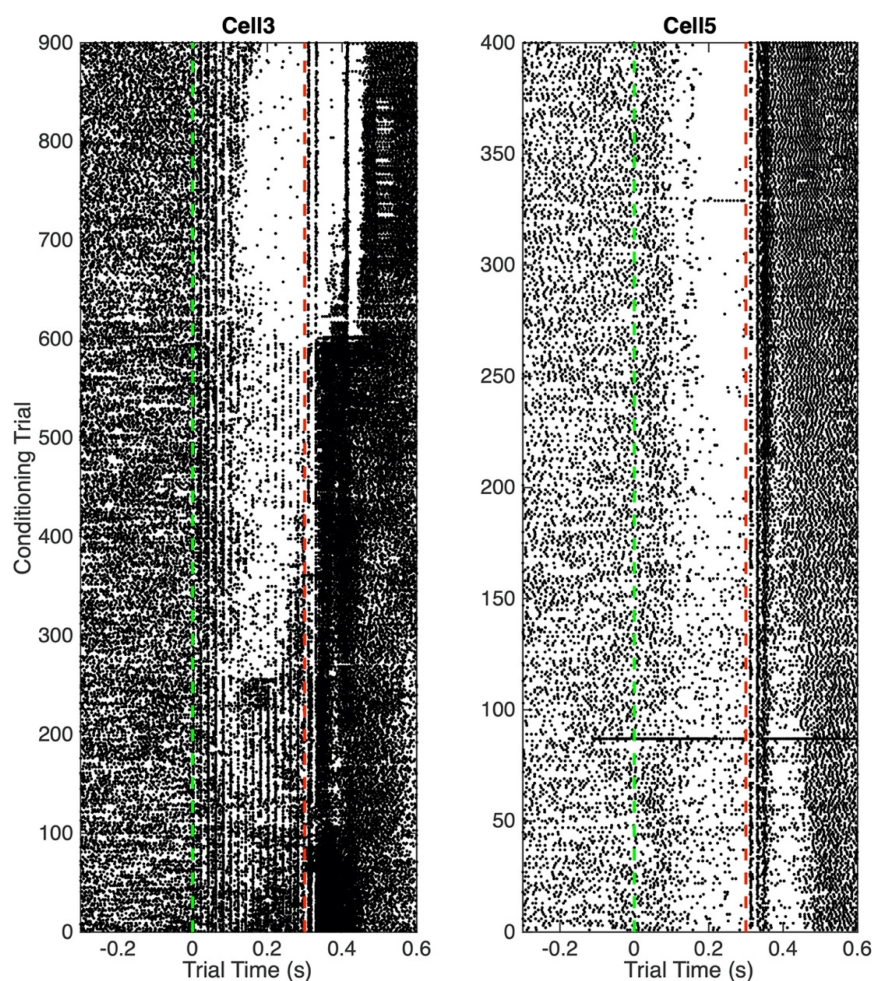


FIGURE 3

Raster plots. Each dot is a spike. Each horizontal line of dots is a trial. Vertical green dashed line indicates CS onset at trial time 0; vertical red dashed line indicates US onset.

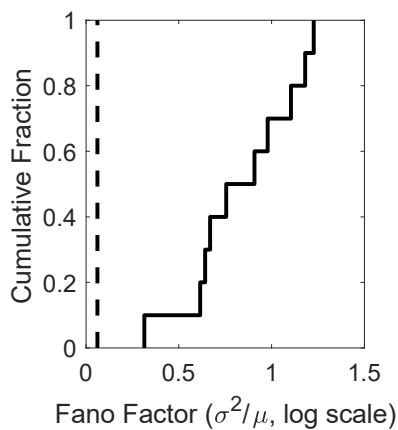


FIGURE 4

The cumulative distribution of the between-trial Fano factors for the 10 cells. The count window was the 1s immediately preceding CS onset. The Fano factor is the ratio of the variance in the counts to their mean. In a stationary Poisson process, this statistic will be close to 1. The dashed vertical line indicates an alpha of 0.01. Given the observed firing rates and sample sizes (numbers of trials), the Fano factor has a 0.01 probability of exceeding this limit if the process is stationary and Poisson (Eden and Kramer, 2010). Evidently, it is far from stationary on the time scale of the inter-trial intervals (15 s).

variance in the spike counts to the mean count, would be close to 1, but in fact the distribution of Fano factors lies well beyond the limits expected from a stationary Poisson process (Figure 4).

The evidence in Figure 4 of a basal firing rate that fluctuates from trial to trial raises the question of the time scale of this non-stationarity. In Figure 5, we give the cumulative distributions of the trial-by-trial Fano factors for the pre-trial firing of each cell. These spike counts came from successive 0.1 s windows in the pre-trial period of each trial, an order of magnitude smaller time scale than that in Figure 4. Because spike recording was turned on at varying intervals prior to CS onset, the number of such windows varied from 15 to 40. The bulk of these distributions tend to fall within the plausible limits for a stationary Poisson process (dashed verticals in each panel of Figure 5), although in several cells a substantial portion of the Fano factors are sub-Poisson (indicating less variance in the spike counts than would be the case if they were generated by a Poisson process). The distribution of interspike intervals is, however, not exponential; they have a much fatter tail (see below, Figure 11).

Variable course of acquisition

The common impression that behaviorally measured conditional responses develop gradually is an artifact of averaging across trials and subjects. The conditional response in most conditioning paradigms—both Pavlovian and instrumental—appears abruptly in most subjects (Gallistel et al., 2004; Papachristos and Gallistel, 2006). Its appearance is best visualized by means of a cumulative record of the

trial-by-trial differences between the rate of responding prior to CS onset and the rate of responding during the CS (Figure 6). The slope of a cumulative record of a sequentially observed variable is the average value of that variable at a given point in its evolution. Early in conditioning—in the naive subject—the slope of the cumulative differences is usually 0 or even negative (because some subjects become wary in the presence of a novel stimulus). When the conditional response appears, the slope of the cumulative record becomes positive.

The advantage of visualizing acquisition by means of a cumulative record is that there is no averaging. Hence, there is no smoothing; the more abrupt the change in behavior, the more abrupt the change in the slope. There are well-established algorithms for objectively identifying changes in slope (Gallistel et al., 2004). We can visualize the emergence of the conditional pause in the firing of a Purkinje cell by making a cumulative record of the difference between the pre-CS firing rate and the firing rate during the CS. And, we can apply to these records, the algorithm for identifying the changes in the slope (Figure 6).

Figure 7 shows the normalized peri-CS histograms computed only from the post-pause-acquisition trials, the trials after the vertical dashed lines in Figure 6. These histograms span the interval from 0.3 s before CS onset (at 0) to the end of the CS-US interval. These histograms give the momentary probability of a spike, defined as the probability of observing a spike within any 1 ms interval. They enable us to estimate three quantities that enter into the computation of an estimate of the pause onset time on a trial by trial basis: (1) the 15 ms wide interval at which the momentary probability of a spike is minimal (the bin with the lowest bar); (2) the momentary spike probability at that low point (the height of the lowest bar); (3) the momentary spike probability over the pre-CS interval (the average heights of the bars to the left of the 0 at CS onset).

Because the offset of pauses during training tends to coincide with the onset of US stimulation, pause offset cannot be estimated on a training trial; only pause onset can be. The Bayesian algorithm for estimating pause onsets operates on a binarized version of the spike train. Trial time is divided into successive 1ms “moments.” The 1ms width of these moments is chosen to be so narrow that at most 1 spike can occur during any one moment. Binning trial time in this way yields a binary string in which there is a 0 in every moment that did not contain a spike and a 1 in every moment that did. Binarization converts firing rates to momentary probabilities: the higher the firing rate, the greater the momentary probability of a spike. Then, the problem of estimating pause onset becomes one of estimating where the momentary probability of a spike increases as one looks back from the time where that probability is minimal (the retrospective sequence).

The algorithm computes the relative likelihood of two stochastic models for the retrospective binary sequence, a model in which the momentary probability is constant, and a model in which there is a step increase in the momentary spike probability

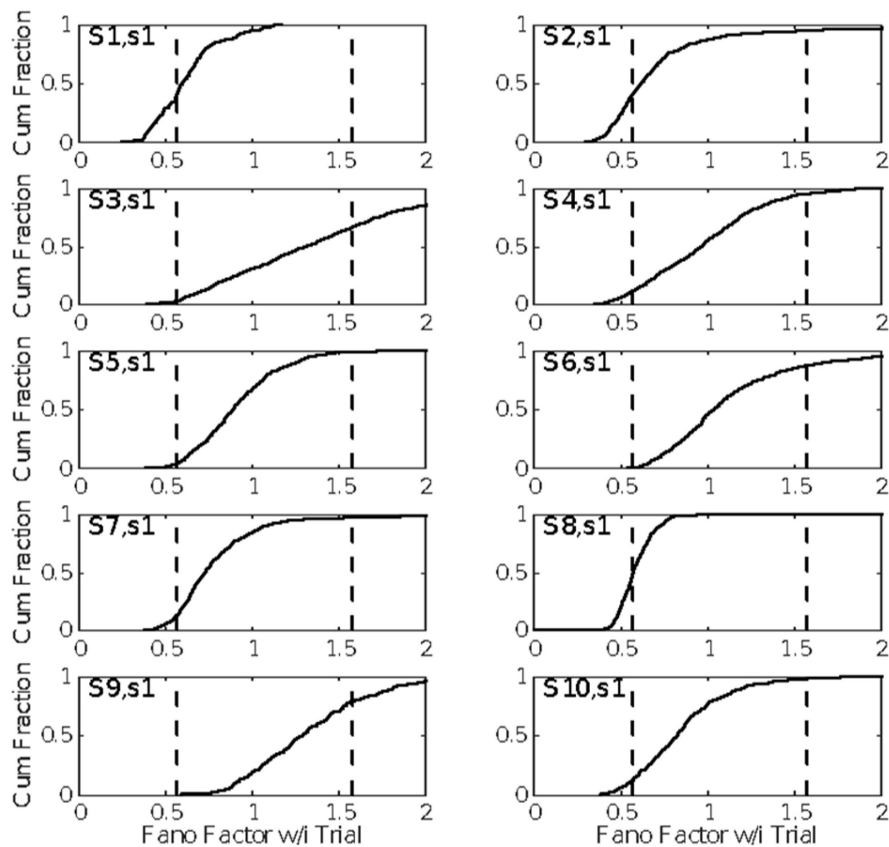


FIGURE 5

The cumulative distributions of the Fano factors for spike counts from successive 0.1 s windows on the spike train preceding each CS onset. The dashed vertical lines indicate the limits for data generated by a stationary Poisson process given the observed spike rates in these windows and the sample sizes (numbers of counts per trial). (For the computation of these alpha levels, see Eden and Kramer, 2010).

as one looks back through the spike train from the low point within the CS. In the course of computing the second model, the algorithm determines the maximally likely location of this step and the strength of the evidence that it in fact exists. The evidence for or against its existence is the log of the odds in favor of the 1-change model as opposed to the no-change model (the null hypothesis in change detection). A log odds of 1 corresponds to odds of 10:1 in favor of the change model; a log odds of -1 corresponds to odds of 10:1 in favor of the no-change model. The log of the odds is called the weight of the evidence; weights of 2 and -2 correspond to 100:1 odds; -3 and 3, to 1,000:1 odds and so on. For the algorithm, see PauseCode.²

Figure 8 graphs pause acquisition statistics for two of the 10 cells. The dashed vertical lines are at the same locations in these plots as in Figure 6, namely, at the estimated trial of acquisition. Cell 5, whose statistics are plotted in the left column, was one of the 4 cells whose pause-acquisition was estimated in Figure 6 to occur at Trial 2, that is, after a single experience

of the CS-US interval. Consistent with this, we see in the top left panel of Figure 7 that in this cell on the great majority of trials, δ_{pre} , the firing rate during the pre-CS interval was higher than δ_{ps} , the firing rate during the pause. The sign of the difference in firing rate was reversed in several early trials, but as training progressed, the trial-to-trial variability in the firing-rate difference decreased markedly. We see in the left middle panel that the evidence for this change in the firing rate was very strong even at the beginning, although it clearly became stronger still as training progressed and the pause became broader. The upper limit on the weight of the evidence (the ordinates of the middle panels) has been set to 5, which corresponds to odds of 100,000:1. The plot rises above this limit on most later trials. Even on the earliest trials, it is not infrequently above this limit. Finally, we see in the bottom left panel that the central tendency of the pause onset latency became shorter as training progressed and the variability in this onset latency decreased.

Cell 6, whose statistics are plotted on the right-hand column in Figure 8 was one of the 6 cells with an estimated pause-acquisition trial greater than 2. In the top-right panel, we see that on trials prior to this estimate, the $\lambda_{pre} - \lambda_{ps}$ difference

² https://osf.io/879pk/?view_only=34820e6bd9584bf486aee56c88725ba4

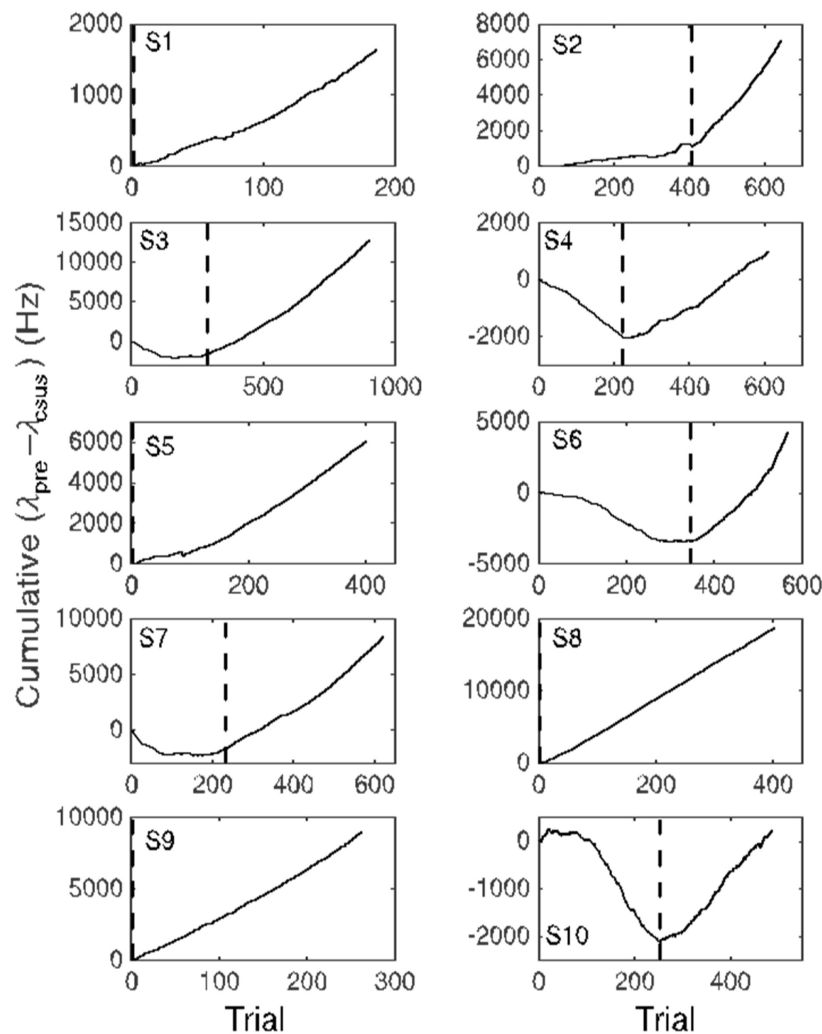


FIGURE 6

Cumulative records of the difference in firing rate between the immediately pre-CS interval equal in duration to the CS-US interval and the CS-US interval. An upward slope occurs when the average firing rate during the CS-US interval is less than during the interval preceding CS onset. Dashed vertical lines indicate the trial beyond which this average difference exceeded 10 Hz. This point is an estimate of the trial at which the conditional pause appeared (trials to acquisition).

fluctuated around 0. In the middle-right panel, we see that the evidence for a change in firing rate was weak and often negative (that is, the odds favored the model in which $\lambda_{pre} - \lambda_{ps} = 0$). For a pause onset to be detected on a given trial, the $\lambda_{pre} - \lambda_{ps}$ difference must be positive and the evidence of a change must exceed 1 (10:1 odds) in favor of a step decrease in firing rate at the estimated location). In the light of the data in the top two panels on the right, we are not surprised to see that, with one exception, pause onsets were not detected until after the dashed vertical. Thus, what we see in these plots is consistent with the estimated trials on which a conditional pause was acquired (dashed verticals in **Figure 6**), and this is true for the other six cells as well.

Two aspects of these plots may seem puzzling: First, some pause onsets are negative. Second, there is sometimes

strong evidence of a change on a given trial but no pause onset is detected.

Pause onsets can be negative because the distribution of inter-spike intervals in the spontaneous firing of Purkinje cells has an extremely long tail. Although the modal inter-spike interval is often less than 10ms, inter-spike intervals longer than 100ms occur with some frequency. The pause-onset latency in a cell trained with a 300ms CS-US interval hovers near 100ms (bottom panels of **Figure 8**). When CS onset occurs soon after the beginning of a spontaneously generated inter-spike interval greater than 100ms, the shut-down in the firing produced by the CS occurs during that spontaneously generated inter-spike interval. In that case, the onset of the pause will appear to precede the onset of the CS.

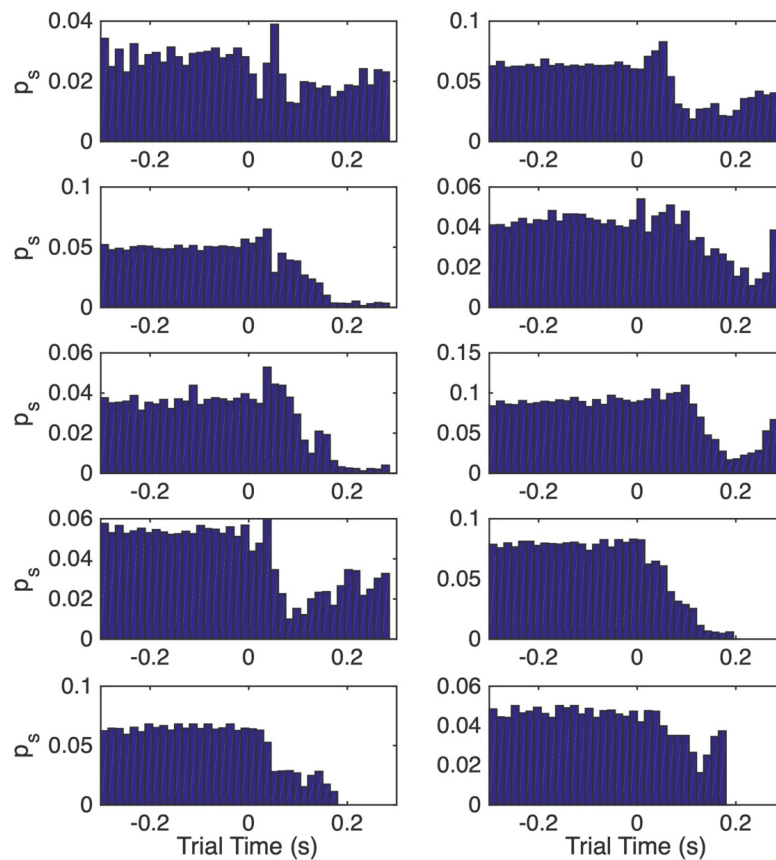


FIGURE 7

Normalized peri-CS histograms computed from the post-acquisition trials. The interval from 0.3 s before CS onset to the onset of the US is subdivided into 15 ms wide bins. The height of the bar in a bin gives the momentary probability of a spike over the span covered by that bin, where momentary probability is the probability of observing a spike within any 1 ms interval.

A pause onset is not detected despite strong evidence of a change in p_s when the algorithm encounters a clear negative step in the $\lambda_{pre} - \lambda_{ps}$ difference when looking backward in the spike train. The computation of the strength of the evidence for a change is oblivious to the sign of the change, but a pause onset is detected only on trials where $\lambda_{pre} - \lambda_{ps} > 0$. On some rare anomalous trials, the firing rate increases during the CS rather than decreasing. On those trials, a pause is not detected.

Pause onset latencies

Figure 9 gives the distribution of pause-onset latencies for the trials after pause acquisition on which a pause was detected.

Discussion

These cellular-level data on trial to acquisition and pause onset latency are broadly consistent with behavioral level data. We postpone the discussion of the data on onset latencies until after the analysis of the next data set, which is much larger, and

has a much wider variation in the CS-US interval. Here, we discuss only trials to acquisition.

Trials-to-acquisition vary greatly between subjects in eye blink conditioning, as in most other forms of conditioning (Gallistel et al., 2004; Papachristos and Gallistel, 2006). In the conditioning of these cells, the inter-trial interval was very short (15s). Trials to acquisition are generally inversely proportional to the inter-trial interval; with intervals this short, the number of trials required often runs into the hundreds (Gibbon and Balsam, 1981; Gallistel and Gibbon, 2001).

It may seem remarkable that a pause often appears after a number of trials so small that the number of trials to acquisition cannot be estimated by a change-detection algorithm, in which case an algorithm for estimating trials to acquisition will set the number at 0. 0 trials to acquisition is analytically impossible. There must be at least one trial before a response based on information communicated only in a trial can be observed. In associative learning protocols that use foot shock, one trial learning is common. In eye blink conditioning, however, the lower end of the trials-to-acquisition range is around 10 trials,

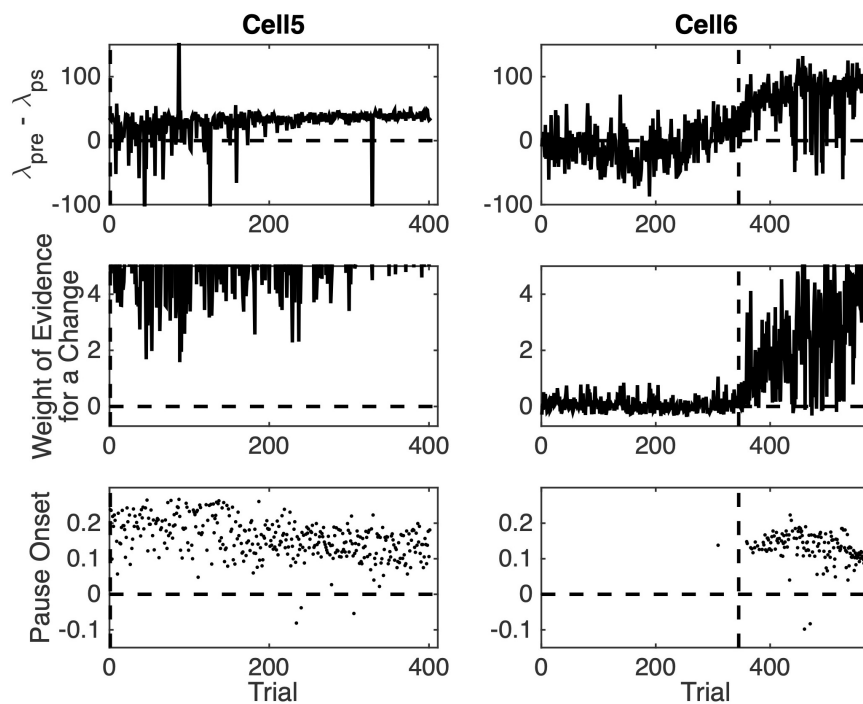


FIGURE 8

Pause statistics for two cells as a function of training trial. **(Top row)** The difference between the pre-CS firing rate and the firing rate during the CS. **(Middle row)** Weight weight of the evidence $\log_{10}(\text{odds})$ for a change in firing rate between the pre-CS interval and the CS interval. **(Bottom row)** Estimated pause onset latency (s).

at least with non-human subjects. Several considerations are relevant in considering what conclusions to draw from the fact that in some preparations there is evidence of a conditional pause after the first training trial. The most important of these considerations is conceptual; it has to do with the difference between a plastic conception of memory-formation in associative learning and an inscriptional conception.

The importance of the Purkinje cell pause-conditioning phenomenon is that it provides neuroscience with an example in which a specifiable quantitative fact gleaned from experience has been localized to the cellular level. It appears necessary to think of this phenomenon in inscriptional terms; the conditioning protocol has inscribed the duration of the CS-US interval into a medium intrinsic to the Purkinje cell (the engram). This conceptual framework differs fundamentally from the framework in which the phenomena of learning and memory are treated in the neurobiological literature, for reasons we now pause to explain.

The neurobiology of learning and memory is focused on synaptic plasticity (Martin and Morris, 2002; Poo et al., 2016). That focus reflects a commitment, witting or unwitting, to a behaviorist conception of learning and memory. In this conception, experience does not inscribe facts; it molds circuits. It alters the brain's wiring by changing synaptic conductances. The changes in the synapses alter signal flow in such a way as

to change the brain's input-output function; they do not encode a fact extracted from experience. Thus, in work focused on mechanisms of synaptic plasticity (Poo et al., 2016, for example), there is no attempt to say how the mechanisms considered could encode a quantitative fact (Gallistel and Matzel, 2013; Gallistel, 2017; Langille and Gallistel, 2020).

The coding question is unavoidable in an inscriptional theory of learning and memory, because the facts (about, for example, interval durations) must be inscribed and read in accord with some code, just as the program for building an organism is inscribed in its DNA in accord with a code and read from that DNA by code-specific molecular machinery. When thinking in inscriptional terms, the notion of memory "strength" makes little sense. A fact is either legibly inscribed or it is not. If the first experience of a CS-US interval does not legibly inscribe the duration of that interval, then there is no way the brain can know that a second experience of the same interval is in fact the same as the first experience. As in anterograde amnesias, every experience of the same duration, no matter how often repeated, is a novel experience of that duration (Milner et al., 1968; Kritchevsky et al., 1988; Siegart and Warrington, 1996). This consideration seems to require the assumption that in all conditioning protocols in which the subject learns that the CS-US interval has a fixed value, single experiences of that interval inscribe in legible form the duration of the CS-US interval. If

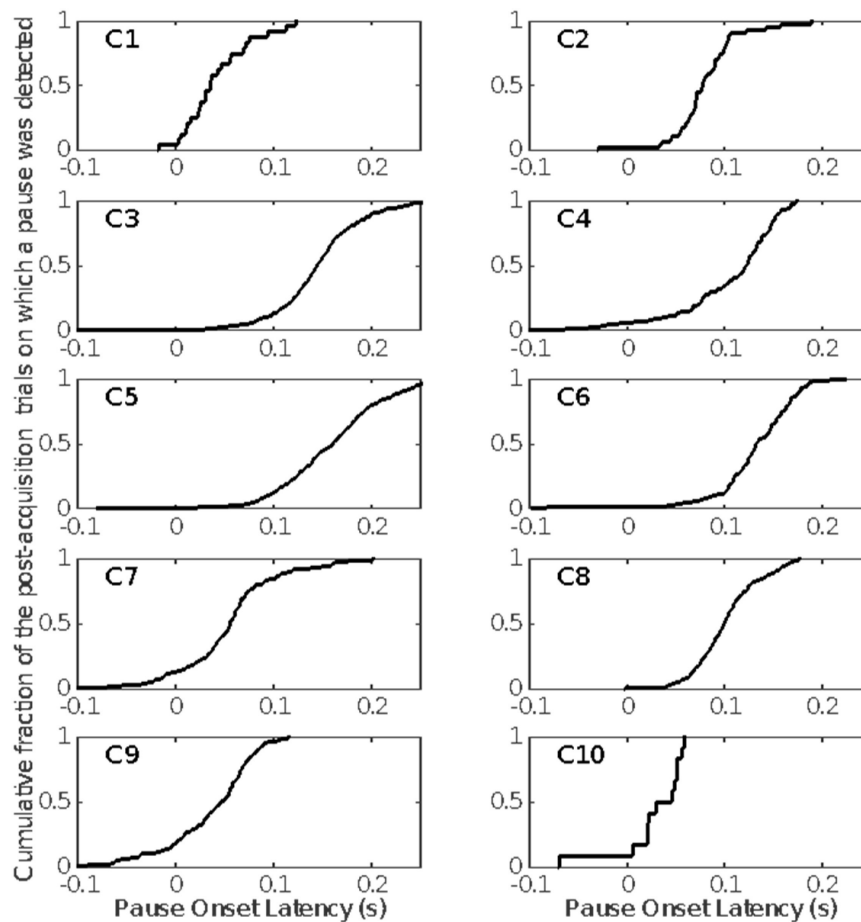


FIGURE 9

The cumulative distributions of pause onset latencies. Included are only those pauses detected after the estimated pause-acquisition trial (Figure 6).

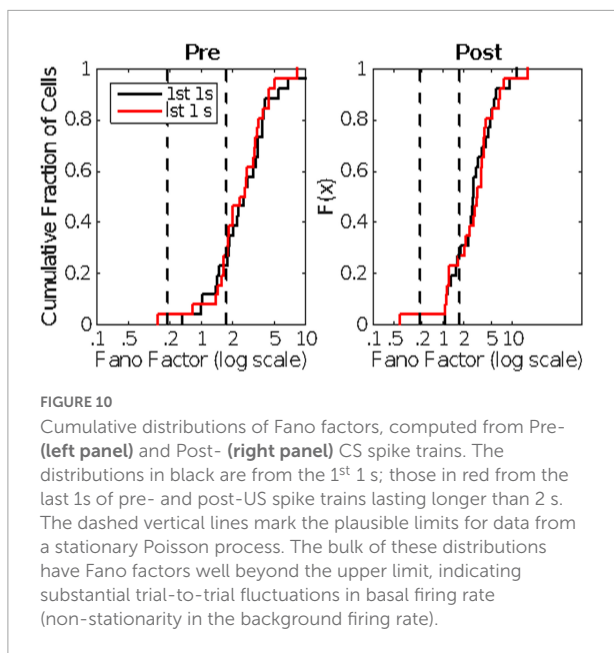
the first experience of that interval did not legibly inscribe its duration, then every subsequent experience of the same interval would be no different from the first experience. There would, therefore, be no way for evidence to accumulate that the CS-US interval was constant from trial to trial; hence predictable. Nor would there be any way for the brain to distinguish trial-to-trial variability in its measurements of a fixed CS-US interval from actual variations in the interval itself, in those protocols where the CS-US interval varies. Rodents do, however, make this distinction (Li and Dudman, 2013; Kheifets et al., 2017). Finally, the results of Ohyama and Mauk (2001) show that rabbits learn the temporal relation between CS and US prior to the point at which they begin to make conditioned responses.

Given this consideration, we are not surprised that evidence of having committed the duration of the CS-US interval to memory is apparent in some cells after a single experience of that interval. In all 10 cells, there was evidence for a further evolution over many trials of its response to the CS (see, for example, the bottom left panel in Figure 7). We assume that it is these

further evolutions and the emergence of a conditional response in more than one Purkinje cell that explains the emergence of a behaviorally observable response.

Experiment 2: Conditional stimulus is stimulation of the dorsum of the paw

The second data set comes from 106 cells recorded from 54 decerebrated ferrets. The CS in the conditioning protocol was pulsatile stimulation at 50 Hz through an electrode on the dorsum of a forepaw. The US was stimulation of a climbing fiber with two 5-pulse bursts of pulses at 500 Hz, with a 10 ms interval between the two bursts. The CS stimulation terminated at US onset. The CS-US interval varied between subjects from as short as 0.15s to as long as 0.45s. The interval from CS onset to CS onset varied from as short as 6s for some subject to as long as 17 s in others. When a clear pause was observed, delivery of the



US was discontinued, and 20 successive probe trials were run with CS alone to obtain the data on which the analyses here reported are based.

In about half the subjects, the electrode was then advanced to find a nearby Purkinje cell that had also been conditioned, and 20 further probe trials were run while recording from that cell. In some cases, as many as 6 trained cells were recorded in a single subject.

Results of the analysis

In the raster plots for these 20 probe trials, it again appears that for many of the cells the basal firing rate fluctuates from trial to trial. We therefore computed the Fano Factors for the spike counts in two pre-CS and two post-CS windows of 1 s width, for all those cells in which the pre-CS and post-CS spike trains were both recorded for more than 2 s. The two windows were the first 1 s and the last 1 s of such spike trains. The cumulative distributions of the Fano factors are shown in **Figure 10**. The pre-CS and the post-CS distributions are the same (compare left and right panels in **Figure 10**), as are the distributions for the first and last 1 s windows (compare black and red distributions within panels).

Seventy-five percent of the Fano factors are beyond the upper limit on a plausible Fano factor from a stationary Poisson process. Moreover, and perhaps more importantly, even for the rare cells for which all 4 Fano factors were within the plausible Poisson limits, the distributions of interspike intervals were not well fit by the exponential distribution that describes intervals generated by a Poisson process. The distributions for these three cells have a fatter tail than the exponential (**Figure 11**). These

properties—an extremely steep rise and a long, fat tail—are more marked in the great majority of the inter-spike interval distributions than they are in the examples in **Figure 11**. It would seem that the endogenous process that generates the high rate of spontaneous spiking in Purkinje cells is not a Poisson process and it is not stationary.

Pause statistics

Using our algorithm for finding pause onsets and offsets (see *PauseCode*),³ we found trial-by-trial pause onsets and offsets for the data sets from each of 106 cells. From the offsets and onsets, we computed the pause widths. We also computed the maximum interspike interval between each pause on and pause off and the latency from pause on to the onset of the longest interspike interval.

The top row of **Figure 12** gives scatter plots of the pause-onset latencies, the pause-offset latencies and the pause widths (the difference between the two latencies), while the bottom row gives the coefficient of variation (CoV) in these statistics. The CoV is the ratio between the standard deviation of a random variable and its mean. In time-scale-invariant measures, measures that obey Weber's Law, the standard deviation in the measure increases in proportion with the mean, so the CoV is constant. We do not graph the fifth basic statistic—the latency from pause onset to the beginning of the longest within-pause inter-spike interval—because most pauses begin with the longest within-pause inter-spike interval, regardless of the duration of the CS-US interval. From this and other aspects of the data, we conclude that the unusually long interspike interval *is* the pause.

Pause statistics scale with the training interval

The most conspicuous aspect of the results in **Figure 12** is that the pause onset and pause offset and the interval between them become progressively longer as the CS-US interval during training increases (top row of **Figure 12**). A second feature is that CoVs for these intervals are constant. In other words, these statistics exhibit scalar variability. Scalar variability is ubiquitous in behavioral timing (Gibbon, 1977, 1992; Gibbon et al., 1984; Gallistel and Gibbon, 2000; White et al., 2000; Simen et al., 2013). It is a manifestation of Weber's Law and of time-scale invariance, both of which are quantitatively important aspects of associative learning (Gallistel and Gibbon, 2000). The range covered by the CoVs of the pause offset latencies is the same as that observed in behavioral experiments on the timing of conditional responses (Gallistel and Gibbon, 2000; Kehoe et al., 2010).

The systematic increase in the central tendencies of the timing quantities and the proportionate increase in their variability are further examples of the many ways in which the quantitative properties of this cellular-level learning

³ https://osf.io/879pk/?view_only=34820e6bd9584bf486aee56c88725ba4

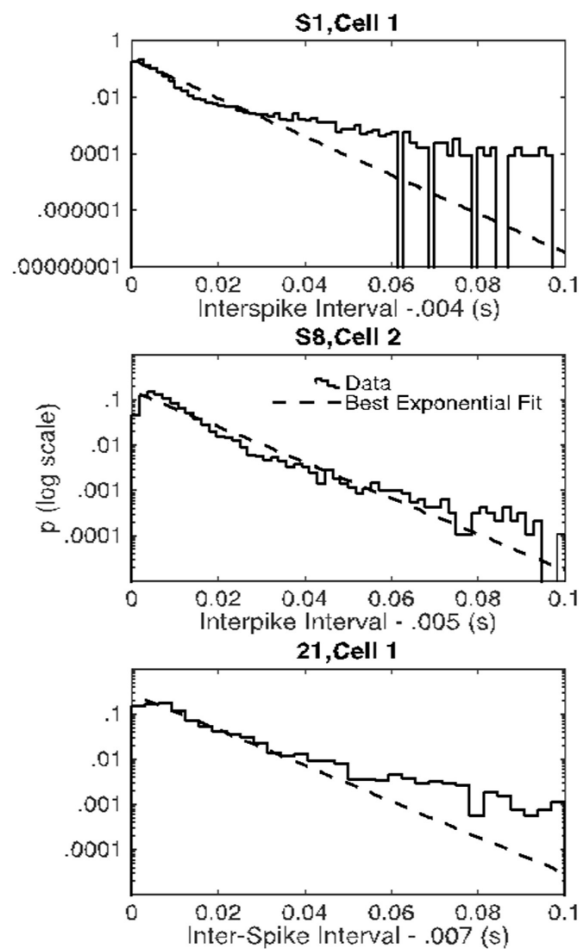


FIGURE 11

Empirical probability distributions of interspike intervals (after subtraction of the minimum interval) in the three cells with Fano factors consistently within the Poisson range (solid curves) and the best-fitting exponential distributions (dashed lines) on semilog. The empirical distributions have fatter-than-exponential tails.

phenomenon match the quantitative properties that are known to obtain at the behavioral level (Jirehned and Hesslow, 2016). This correspondence between quantities measured at the cellular level and corresponding quantities measured at the behavioral level stands in marked contrast to the situation with LTP (long term potentiation) and STDP (spike-timing-dependent plasticity). None of the quantitative properties of these cellular level phenomena agree with the behaviorally determined quantitative properties of associative learning (Martin and Morris, 2002; Gallistel and Matzel, 2013).

Pause onset latency can be extremely short

The onset latencies are remarkably short when cells are trained with a 0.15s CS-US latency. This latency is close to the shortest CS-US interval that will produce a conditional eye blink (0.1s), which is also the shortest interval that will produce a conditional pause in the Purkinje cell (Schneiderman and Gormezano, 1964; Salafia et al., 1973;

Jirehned and Hesslow, 2016). The median of the median onset latencies in the group trained with a 0.15s CS-US interval is slightly less than 20 ms. Thus, in 50% of the cells, half the pauses began before the delivery of the second pulse in the train of CS pulses that was delivered to the dorsum of the forepaw. In the much more numerous group of cells trained with a 0.2s CS-US interval, the median of the median pause onset latency was 40ms and the median of the 1st quartiles was just over 20 ms. Thus, on half the trials in this condition, the pause began at or before the delivery of the 3rd pulse in the train of CS pulses, and on slightly less than 25% of the trials it began at or before the delivery of the 2nd pulse in the CS stimulation of the forepaw.

Pause onsets and offsets are step-like

The first inter-spike interval within the pause is more often than not the longest inter-spike interval within the pause. This is

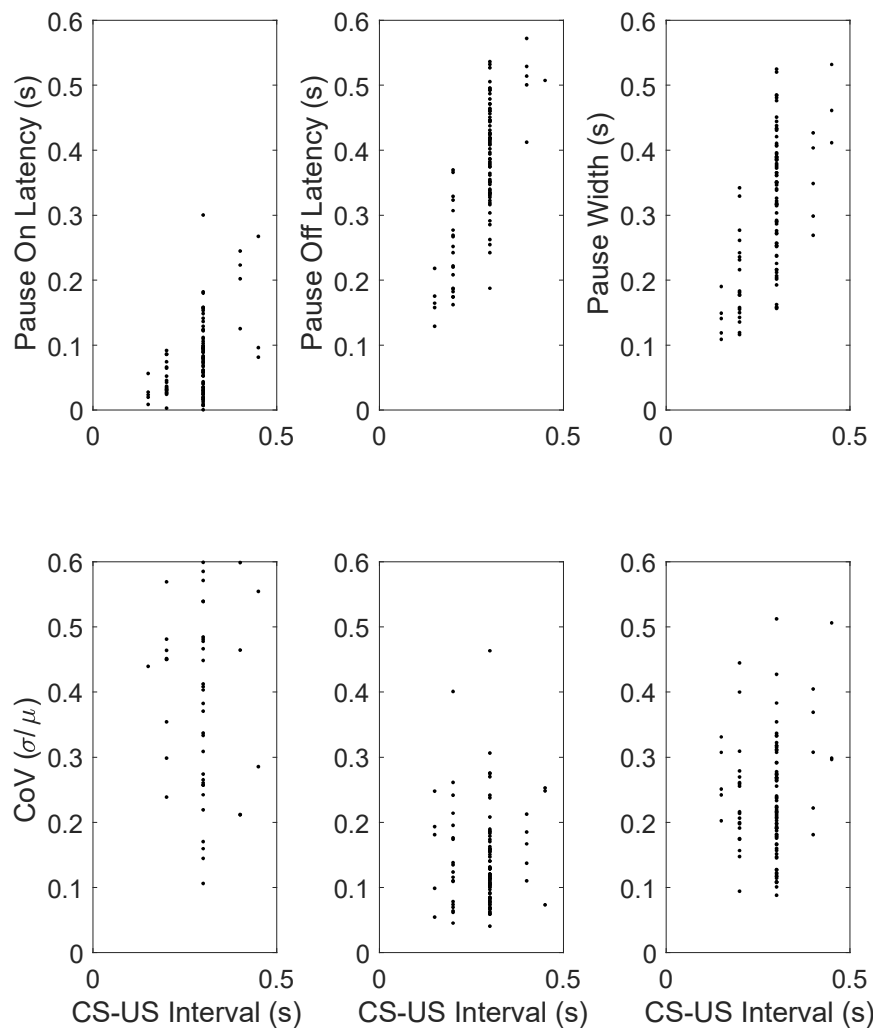


FIGURE 12

(Top row) Scatter plots of mean pause-onset latencies, mean pause-off latencies and mean pause widths as a function of the CS-US training interval. (Bottom row) The coefficients of variation.

a major reason for our conclusion that on any given trial a single unusually long interspike interval *is* the pause. This hypothesis explains why the distributions of pause widths and of the longest inter-spike intervals within the pause are so similar, as may be seen in **Figure 13**, which plots the cumulative distributions of the pause-width-distribution quartiles (left columns) and the cumulative distributions of the quartiles of the longest-within-pause inter-spike interval distributions (right column). The onset latency and duration of this unusually long inter-spike interval are determined by the memory of the previously experienced CS-US intervals (the engram).

To check whether there was evidence of any lengthening of the inter-spike intervals after CS onset but before what our algorithm identified as the onset of the pause, **Figure 14** give scatter plots for the successive inter-spike intervals encountered when looking backward from pause onset to CS onset in a

representative sample of cells trained with a 0.3s CS-US interval. These plots do not suggest any reliable upward trend in the inter-spike intervals between CS onset and pause onset. These retrospective plots are only possible for cells in which there are trials with two or more spikes within the CS prior to the estimated locus of pause onset, which is why we confined this analysis to cells conditioned with CS-US intervals ≥ 300 ms. The complete set of such plots is available in this repository (see text footnote 1).

The question arises whether the unusually long interspike interval is the culmination of a sequence of lengthening interspike intervals or whether, as we have suggested, the pause simply *is* the unusually long interspike interval. As a more rigorous check on whether the interspike intervals tend to grow longer as the appearance of the unusually long interspike interval draws nearer, we computed the linear regression of

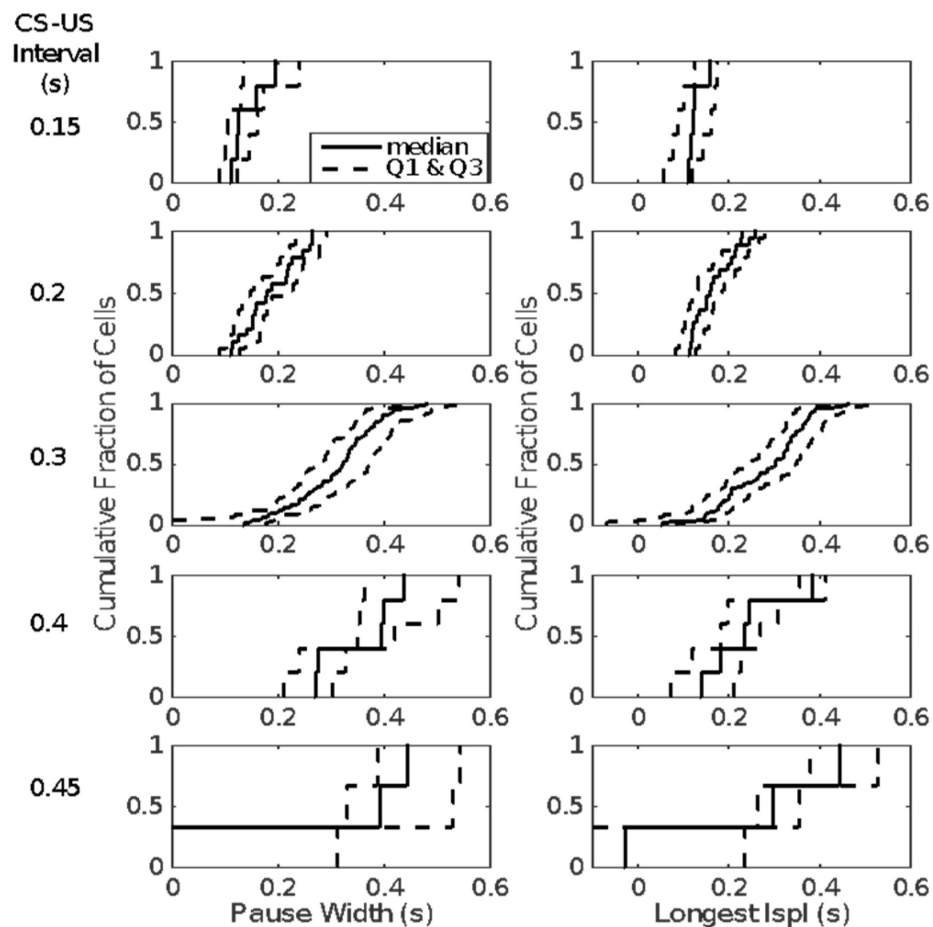


FIGURE 13

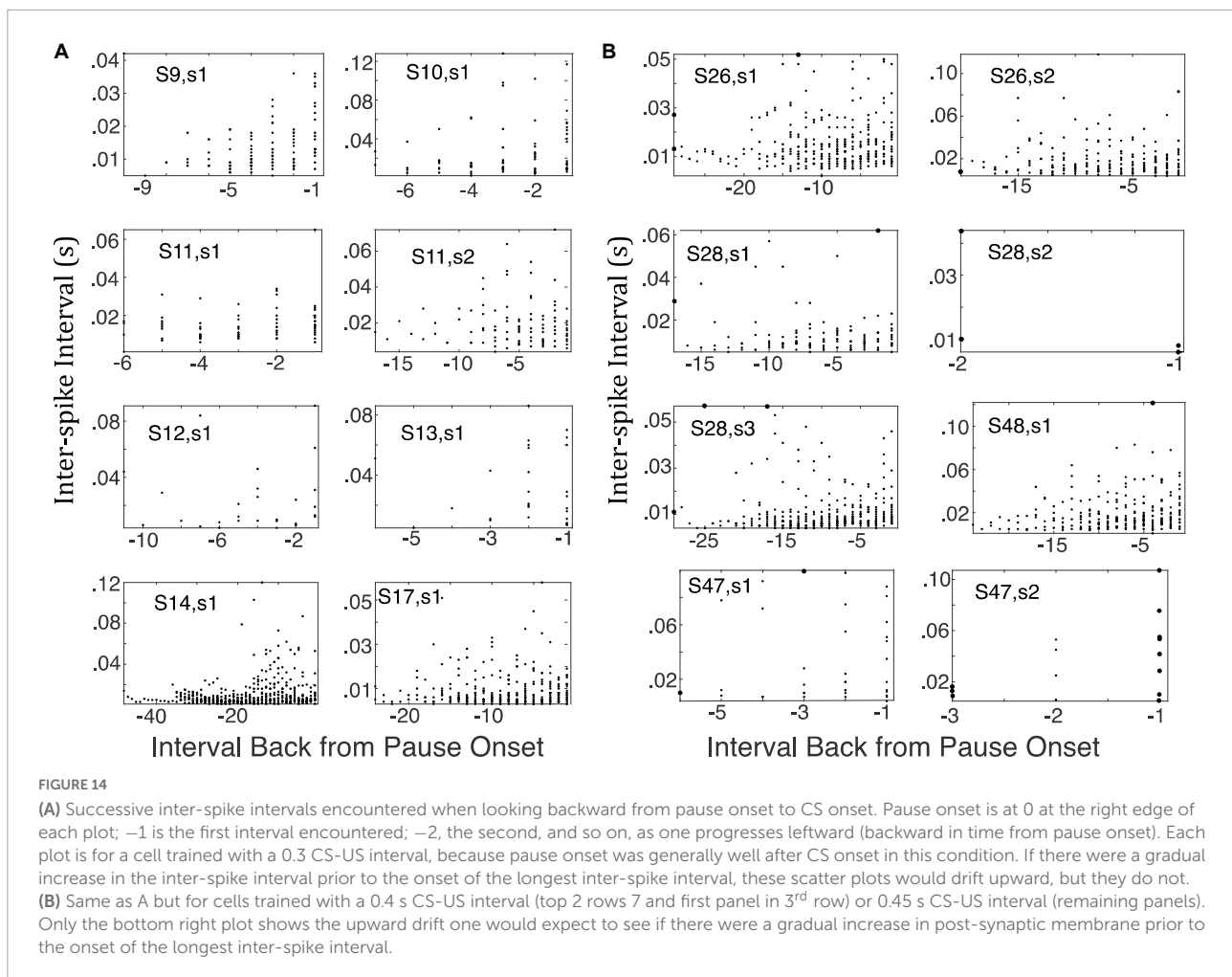
Quartiles of the within-group distributions of pause width (left columns) and longest within-pause inter-spike interval (right column). Cells are grouped by the CS-US interval during their conditioning (given to left of each row). The second quartile (the median) is plotted with a solid line; the first and last quartiles with dashed lines.

the interspike intervals backward from the onset of the longest interspike interval within the pause to the onset of the CS. We did this for all those trials in the CS-US ≥ 0.3 s conditions in which there were at least 5 interspike intervals between CS onset and the estimated onset of the pause. **Figure 15** gives the cumulative distribution functions for the slopes of these regressions, for the lower limit on the slope, and for the variance explained. The bulk of the slopes are positive (**Figure 15**, top), which is to say that interspike intervals farther back in the retrospective sequence (closer to CS onset) tend to be *longer* than those that are earlier in the retrospective sequence (closer to the pause onset). This is the opposite of what one expects if the interspike intervals get progressively longer as the onset of the longest approaches. The tendency is, however, very weak, because in 75% of the regressions, the lower confidence limit on the slope is negative (**Figure 15**, middle)—thus, the confidence interval includes 0—and 80% of the regressions explain less than 7% of the variance (**Figure 15**, bottom). In short, there is no

tendency for the inter-spike interval to grow longer as the onset of the pause draws nearer; the very weak and unreliable tendency that exists is in the opposite direction.

We also made plots like those in **Figure 14** but taking the onset of the longest interspike interval within the CS as the 0^{th} spike, so a spike that preceded it but still fell within the CS defined the first backward interspike interval and so on. These plots may also be viewed in the same repository (see text footnote 1). They, too, give no consistent indication of a decline in momentary spike probability prior to the onset of the longest interspike interval.

We conclude that the conditional pause in the firing of the cerebellar Purkinje cell consists more often than not of a single unusually long inter-spike interval whose onset and offset latencies are a scalar function of the CS-US training interval. There is no sign of the graded increase in inter-spike intervals that would be expected if a gradually strengthening inhibitory



synaptic input increased postsynaptic membrane polarization in a temporally graded manner.

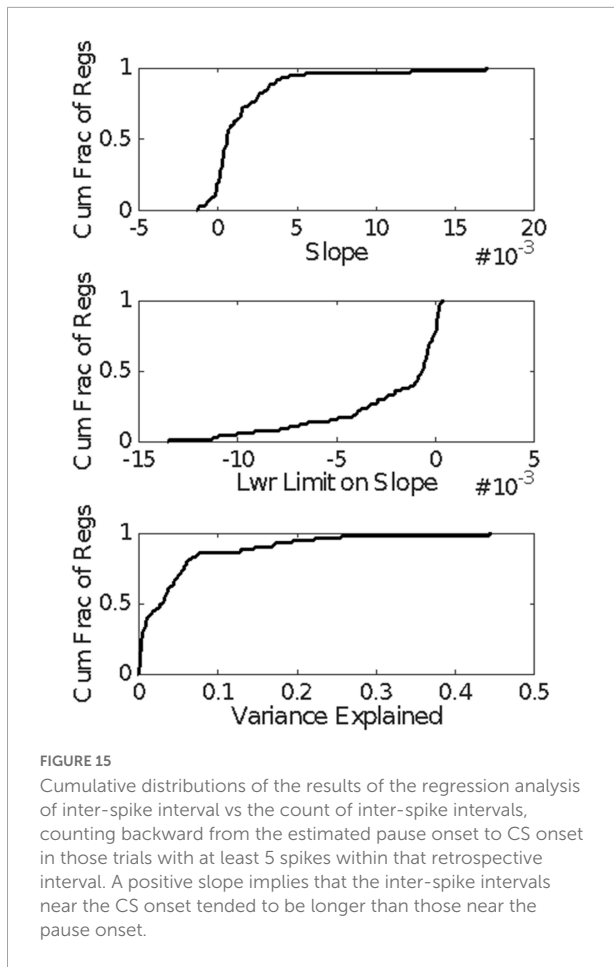
Correlations among pause parameters

Figure 16 shows for each CS-US interval group the pairwise correlations among the 4 pause parameters: pause onset, pause offset, pause width and the longest within-pause inter-spike interval. The structure is the same regardless of the CS-US training interval (compare across panels in Figure 16). The correlation between pause onset latency (\uparrow) and pause offset latency (\downarrow) is highly variable between cells within a group, but the central tendency is close to 0. By contrast, the correlation between pause width (W) and pause onset latency is consistently negative, often strongly so: a late onset predicts a short pause. Because the pause very often begins and ends with the beginning and end of the longest within-pause inter-spike interval (M), it is not surprising that a late onset also predicts that the longest inter-spike interval within the pause will be relatively short. In this same light, it is also not surprisingly that pause width and the longest within-pause inter-spike interval are strongly and positively correlated with pause-offset latency,

and very strongly correlated with one another. We defer to the General Discussion a discussion of the implications of these correlations.

Experiment 3: Conditional stimulus is stimulation of the parallel fibers

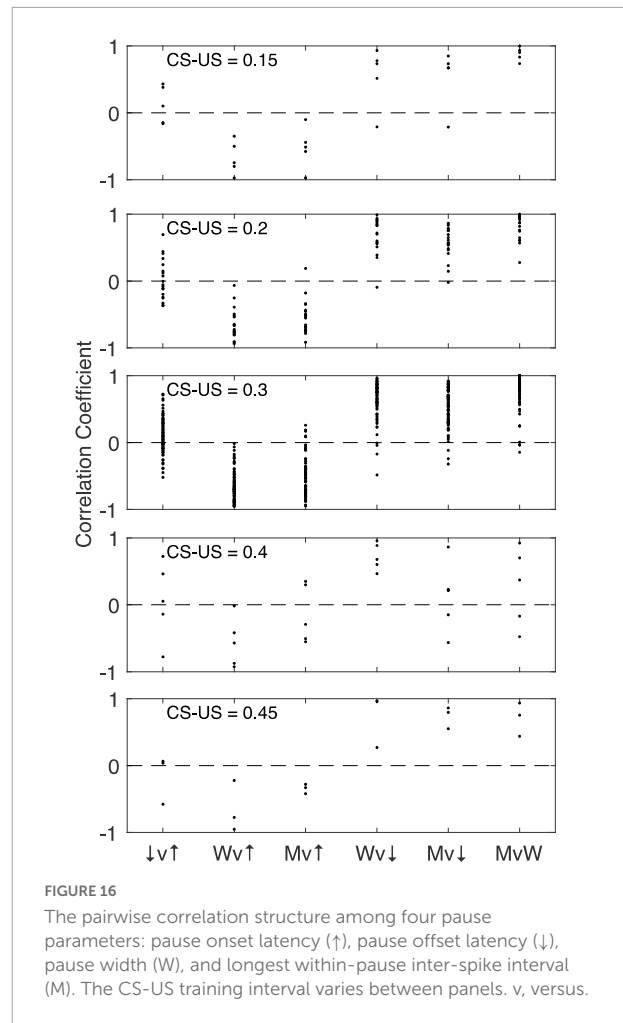
In this experiment, the CS was direct pulsatile electrical stimulation of the parallel fiber input to the Purkinje cell at 50 or 100Hz (0.1ms pulse width), and the US was, as usual, two very short bursts of very high frequency (500Hz) stimulation of the climbing fiber. In this experiment, there was direct control of the presynaptic signal to the Purkinje cell. In previous experiments, the CS signal was generated by stimulation delivered at a remove of two or more synapses from the Purkinje cell. Hence, it was possible that neurons intervening between the site of CS stimulation and the Purkinje cell provided a presynaptic signal with a rise and fall that might explain the pause. In



this experiment, the presynaptic signal—the signal seen at the synapses between the parallel fibers and the Purkinje cell—was under direct experimental control.

We here analyze 22 cells from this experiment. Nine of them were conditioned with a CS-US interval of 0.15s but a CS duration of 0.3s. In other words, CS offset was not coincident with US onset during training; it occurred well after the US. Therefore, in the 20 probe trials with no US, which followed the conditioning, and which provide the data we here analyze, CS offset was not coincident with the time at which a US was anticipated but failed to occur. Thus, the termination of CS stimulation did not play a role in the generation of the pause offsets—the recovery of spontaneous firing at the time when a US was anticipated. The recovery occurred well before the termination of the CS stimulation.

Five of the 22 cells were conditioned with CS-US intervals of 0.2s but CS durations of 0.8s. Again, in these 5 cells, the termination of CS stimulation occurred long after the time at which a US was anticipated. Two more cells were conditioned with the same CS-US interval (0.2s) and with CS termination at US onset.



Finally, six cells were conditioned with CS-US intervals of 0.3s and US onset at CS termination.

Results

The most striking thing about the results is their similarity to the results obtained with CS stimulation delivered at a greater remove from the immediately pre-synaptic parallel fiber projection. **Figure 17** give examples from the three different CS-US interval groups. Figures like these for all 23 cells are in the repository (see text footnote 1).

Figure 18 gives scatter plots of the pause-on latencies, the pause-off latencies and the pause widths (top panel) and their coefficients of variation (bottom panel). As previously explained, to the extent that the variation is time-scale invariant—that is, to the extent that these measures obey Weber's Law—the CoV will be constant. **Figure 19** plots the pairwise correlations for 4 pause statistics: pause-on latency, pause-off latency, pause width, and the longest within-pause inter-spike interval.

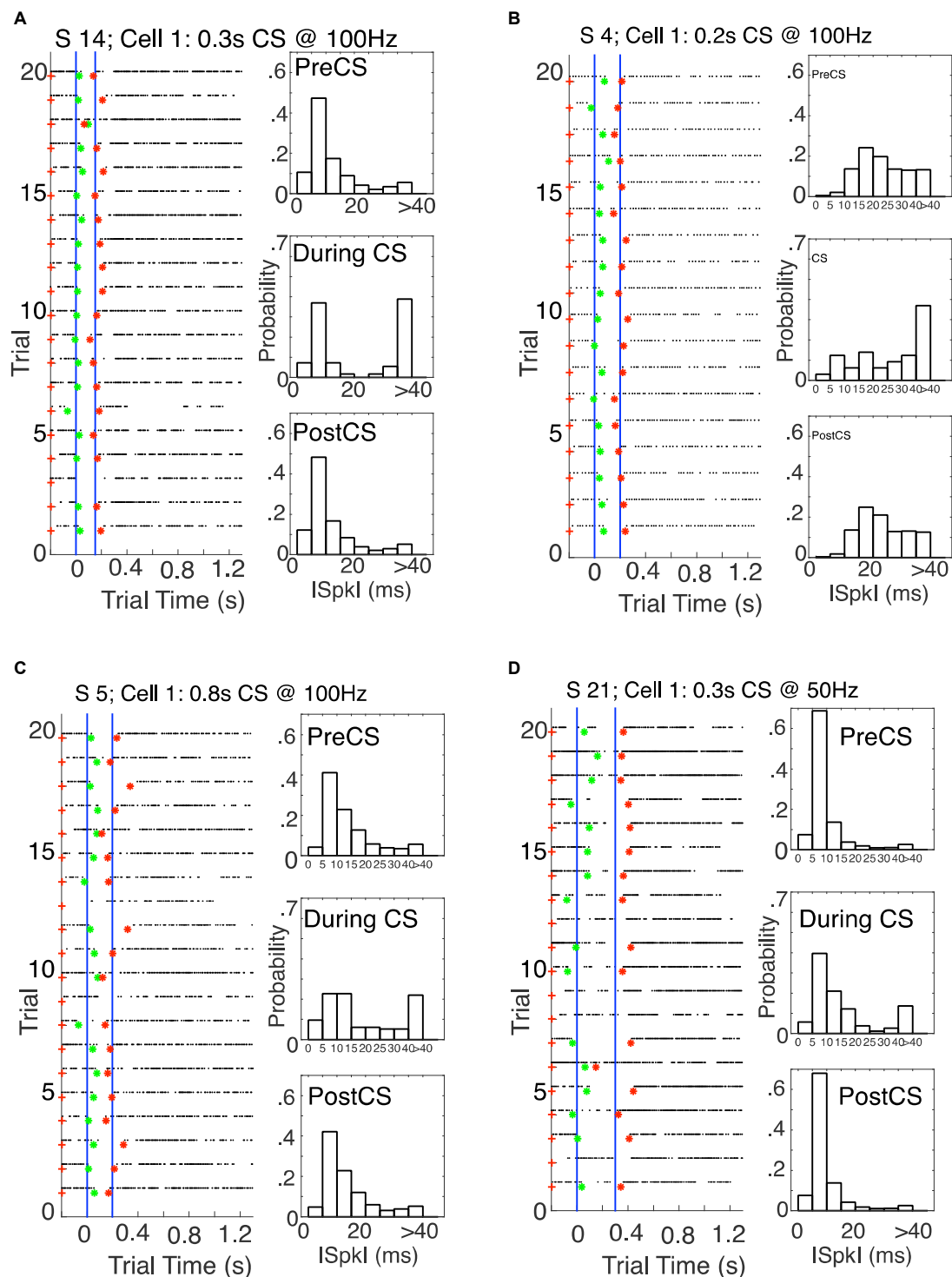


FIGURE 17

(A) Left: Raster plot from 20 probe trials (no US trials), with pause onsets (green asterisks) and offsets (red asterisks) found by the algorithm. The blue verticals mark the CS onset time and the US onset time during training. The CS-US interval was 0.15 s. The CS duration was 0.3 s—twice the CS-US interval—both during training and on these probe trials. Right: Probability distribution functions pre-, during-, and post-CS. (B) The CS-US interval was 0.2 s, as was the CS duration during training and on these probe trials. Thus, for this cell, CS offset during training coincided with US onset. (C) The CS-US interval was 0.2 s, but the CS duration during training and on these probe trials was 0.8 s, four times as long as the CS-US interval. (D) The CS-US interval was 0.3 s, as was the CS duration. Thus, for this cell, CS offset during training coincided with US onset.

The general conclusion from this experiment is that when the CS signal arriving at the Purkinje cell is produced by direct pulsatile electrical stimulation of the immediately presynaptic afferents to the Purkinje cell, the quantitative characteristics of the pause are the same as when the pause is elicited by a sensory CS (stimulation of the dorsum of the paw). This conclusion strongly suggests that mechanisms intrinsic to the Purkinje cell itself determine the quantitative properties of the learned pause in its firing triggered by the onset of parallel fiber input, because the pause is in every way the same under conditions where it is unlikely that there is any time-varying input to the Purkinje cell during a CS.

General discussion

Agreement between behavioral measurements and cellular measurements

When attempting to establish the material basis for a mechanism known only from its behavioral effects, it is essential to establish a quantitative correspondence between properties of that mechanism established by measurements based only on its behavioral effects and properties measured by “more direct” non-behavioral means that bring one closer to the presumed

locus of the unknown mechanism. For example, when Du Bois-Reymond asserted that the “action current” (now called the action potential), which he had discovered in nerve, was the physical realization of the nerve impulse (Du Bois-Reymond, 1848), it was clear that, for his hypothesis to be true, the velocity of the action potential had to be the same as the velocity of the nerve impulse. At about the same time as Du Bois-Reymond did his electrophysiological work, Helmholtz, his friend and colleague in the laboratory of Johannes Müller, measured the velocity of the nerve impulse in frog motor nerve and human sensory nerve (Helmholtz, 1850, 1852), using the difference in reaction time method, which remains a staple of cognitive neuroscience (Luce, 1991). In 1871, a student of Du Bois-Reymond did the behavioral measurements and the electrophysiological measurements on the same preparation (the frog sciatic-gastrocnemius preparation) and found the velocities to be the same within the errors of measurement (Bernstein, 1871), as required by his advisor’s hypothesis.

In attempting to establish the material basis of memory, the same considerations apply (Gallistel et al., 1981): the quantitative properties of a putative cellular level manifestation of the engram must align with the quantitative properties established by behavioral experiment. Electrophysiologically measured synaptic plasticity fails to satisfy this requirement: No measured property of Long Term Potentiation (LTP), Long Term Depotentiation (LTD) or Spike Timing Dependent

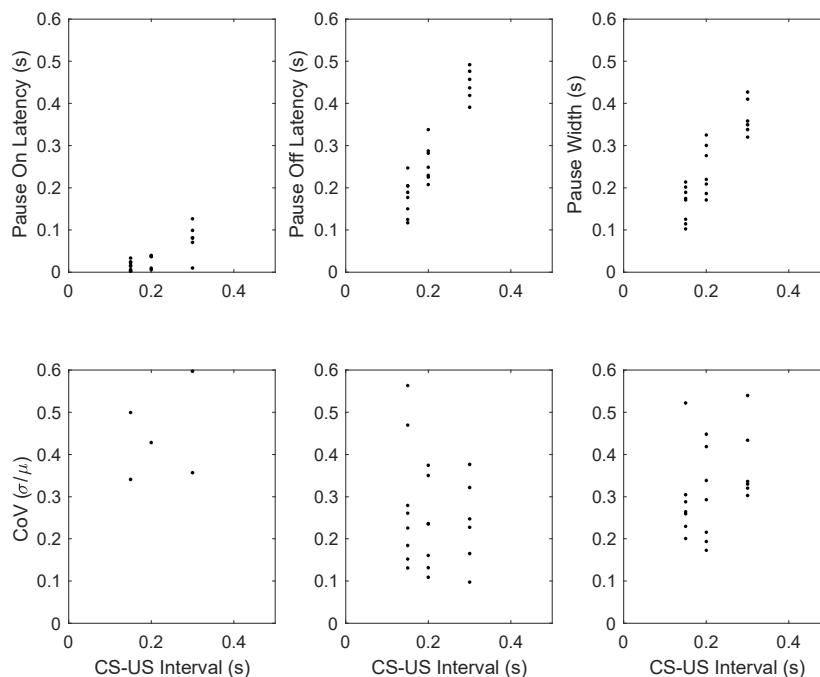


FIGURE 18

Mean pause-onset latencies as a function of the CS-US interval during training (**upper panels**) and the CoVs in the onset latencies as a function of the CS-US interval (**bottom panels**). The flat CoV plot implies that the variability scales with the mean, which is Weber’s Law.

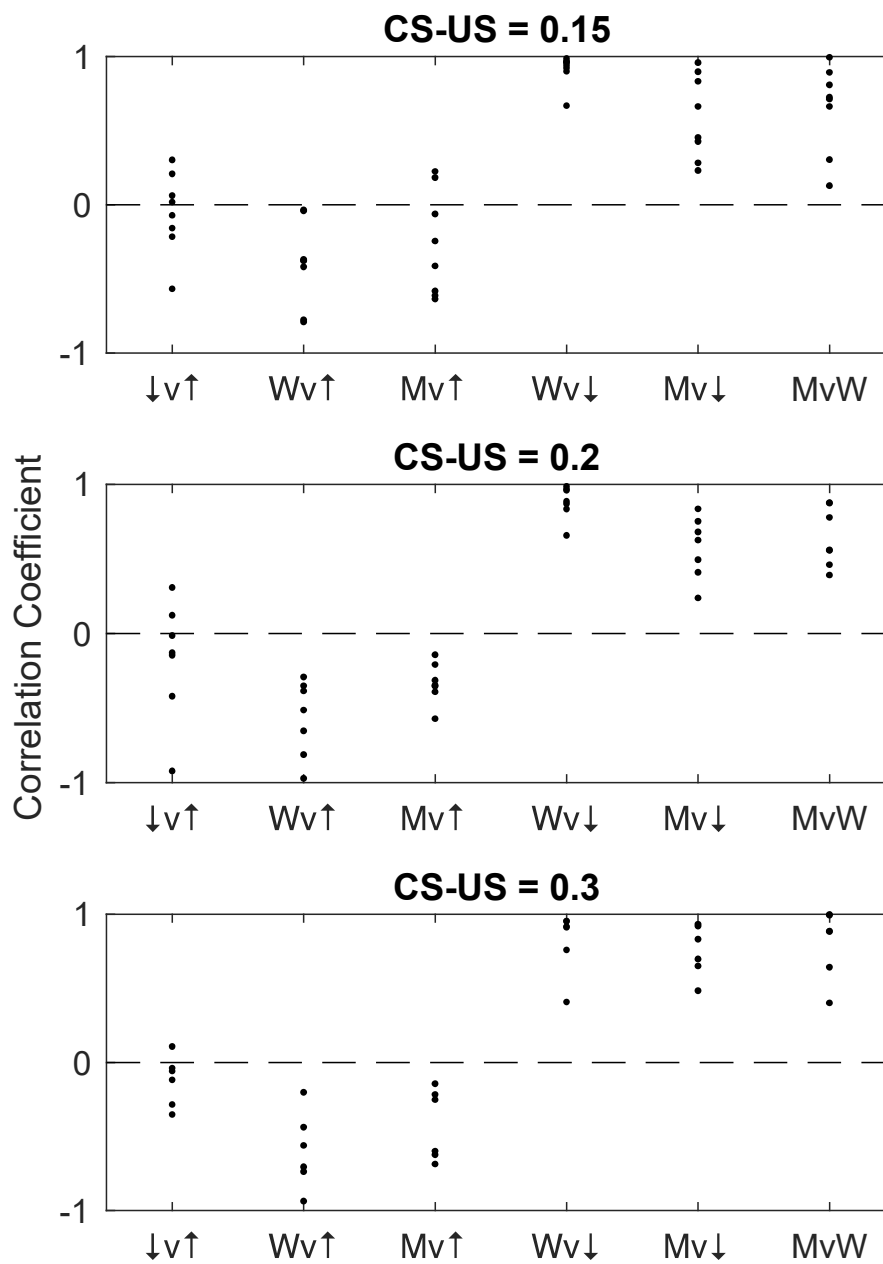


FIGURE 19

The pairwise correlations of 4 pause parameters: pause-on latency (\uparrow), pause-off latency (\downarrow), longest within-pause inter-spike interval (M) and pause width (W). The pattern is the same as that seen in [Figure 16](#), v, versus.

Plasticity (STDP) corresponds to any behaviorally measured property of associative learning ([Gallistel and Matzel, 2013](#)).

The only electrophysiologically measurable phenomenon whose quantitative properties align with the behaviorally established properties of the corresponding associative learning phenomenon is the conditional pause in the spontaneous firing of the cerebellar Purkinje cells, the cells that have been shown to control the timing of the conditional eyeblink

([Heiney et al., 2014](#); [Johansson et al., 2016](#)). [Jirehned and Hesslow \(2016\)](#) review and document the following quantitative correspondences: The numbers of trials required for the acquisition of the conditional response (CR) fall, in both cases, within the same range, as do the numbers required for its extinction. In the cellular preparation as in the behavior of the intact subject, CS-US intervals shorter than 80-100 ms do not induce a CR. In both, reacquisition of the CR

following its extinction occurs much more rapidly than the original acquisition. Preliminary results obtained by one of us (Johansson) suggest that lengthening the intertrial interval causes the CR to appear after fewer trials, as it does for the behavioral CR in the intact rabbit (Gallistel and Gibbon, 2000, Figure 10). And, of course, the timing of the cellular CR depends on the CS-US interval in the same way as does the timing of the behavioral CR, and the offset of the conditional pause occurs at approximately the latency at which the US is expected, which is the time at which lid or membrane closure attains its maximum.

The results we here report add to the list of quantitative correspondences. They show that the CoV for the offset latency in the conditional firing pause of Purkinje cells in the C3 microzone of the decerebrate ferret overlaps the range observed in the CR of the intact rabbit (White et al., 2000), which is 0.12 (SD = 0.045) —see bottom middle panels of Figures 12, 18: median 0.22; (inter-quartile interval = 0.18–0.29). Given that the cellular data come from decerebrate ferrets while the behavioral data come from intact rabbits, this may perhaps be regarded as a reasonable correspondence. It is, however, clearly desirable that both the cellular and the behavioral measurements be made on the same preparations. Also, of course, if the between-cell sources of variance are independent and if the behavioral variance depends on the pooling of the signals from n cells, then the behavioral standard deviation will be smaller than the cellular standard deviation by the square root of n .

Duration engrams store Shannon information

Pavlovian conditioning protocols play a fundamental role in research dedicated to discovering the neurobiological realization of the engram. In contemporary theorizing about the engram in Pavlovian conditioning, the engram does not store Shannon information (Grossberg, 1991; Grossberg and Schmajuk, 1991; Meck, 2003; Mauk and Buonomano, 2004; Yamazaki and Tanaka, 2009; Bareš et al., 2018; Hardy and Buonomano, 2018). The engram is a Hebbian synapse that connects a state triggered by the conditional stimulus to a motor output.

In these models, the lag between conditional stimulus and the CS-conditional response that gives the CS-conditional response its anticipatory character is attributed to an innate dynamics of temporal “grandmother cells” excited by the CS. (A ‘grandmother cell,’ aka a “Jennifer Aniston neuron” is a neuron that represents a complex but specific concept; the problem being that such concepts are potentially infinite in number, as are the number of different durations to which brains may be sensitive. On the kind of theory satirized, we respond to our grandmother because we have neurons that are selectively excited by her and only her.) Temporal grandmother cell theories of timing posit a spectrum of neurons whose firing rates in response to CS input rise and fall with differing

latencies (Grossberg and Schmajuk, 1991; Ludvig et al., 2008; Gershman et al., 2014; Buonomano, 2017). The associative process operating on Hebbian synapses selectively connects the grandmother cells whose peak firing latency matches the CS-US interval to the conditional response. Whether one finds this kind of theory plausible or not, the important thing to note is that the connection itself—the Hebbian synapse (the engram)—does not encode anything (Gallistel, 2017). It is not a symbol for the duration of the CS-US interval nor for anything else about the subject’s conditioning experience (Langille and Gallistel, 2020; Gallistel, 2021). Therefore, it does not store Shannon information. Nor is it read by subsequent CS inputs in the sense in which the Shannon information stored in a computer register is read in the course of computations that operate on that information. There are no such computational operations in conventional neurobiological thinking about the engram, because, in that thinking engrams are not the symbols for quantities on which neurobiologically realized arithmetic operations may operate.

The informationless conception of the duration engram is not consistent with the experimental facts on the role of temporal information in Pavlovian conditioning (Balsam et al., 2006; Balsam and Gallistel, 2009; Gallistel and Balsam, 2014; Kalmbach et al., 2022). The ratios between remembered durations and differences in remembered intervals are critical determinants of the conditioned behavior (Matzel et al., 1988; Barnet et al., 1997; Denniston et al., 1998; Gallistel and Gibbon, 2000; Arcediano and Miller, 2002; Balsam et al., 2010; Ward et al., 2012, 2013; Kalmbach et al., 2019). The learning rate is a scalar function of this ratio; the greater the ratio, the faster subjects learn over most of its range, until the ratio approaches 1, the value at which the CS provides no information about the rate of reinforcement, at which point the rate of learning becomes 0 (Gibbon and Balsam, 1981, Figure 7.2, p. 224). These ratios and intervals would appear to be extracted from remembered experience by arithmetic operations on temporal maps and remembered durations (Honig, 1981; Taylor et al., 2014; Chandran and Thorwart, 2021; Namboodiri and Stuber, 2021).

The informationless conception of the Pavlovian engram is also not consistent with the experimental facts about the conditional pause in the spontaneous firing rate of the cerebellar Purkinje cell, the pause whose duration controls the timing of the conditional blink (Medina and Ruffolo, 2014; Johansson et al., 2016). The experiments in which the CS signal is produced by direct stimulation of the parallel fibers appear to rule out engramless models of timing. The crucial assumption in these experiments is that the parallel fiber input seen by the Purkinje cell directly reflects the train of evenly spaced stimulating pulses delivered to the parallel fibers. If that is the case, the dynamics of presynaptic circuits are irrelevant, because the experimenter has gained control of the relevant presynaptic input to the Purkinje cell. In that case, the experiment insures that an appropriately

timed signal is not delivered to the Purkinje cell by a presynaptic signal from an innate timing mechanism. Given that a signal indicative of the CS-US interval is not present in the parallel fiber input, the timing of the CS-US interval, the encoding and storing of its duration, and the generation of an appropriately informed pause duration on subsequent occasions occur within the Purkinje cell itself, which is the first point at which the CS onset signal and the US signal converge (Johansson, 2019).

That parallel fiber input evokes the conditional pause in the critical parallel-fiber-stimulation experiments is strongly implied by two pharmacological results cited in our introduction: (1) Blocking the mGluR7 receptor in the post-synaptic side of the parallel-fiber-to-Purkinje cell synapse blocks the pause. (2) Blocking the known inhibitory inputs to the Purkinje cell with a general-purpose GABA blocker (gabazine), given in a dose that blocks the very strong inhibitory effect of off-beam stimulation, does not block the elicitation of the conditional pause.

Also relevant is that, to our knowledge, neither the granule cells from which the parallel fibers originate, nor any other neurons in the cerebellum have been shown to exhibit the properties required of the temporal grandmother cells that have been postulated to control the timing of the conditional response.

Given the far-reaching implications for further research of the conclusion that there is an engram for the CS-US interval intrinsic to an intracellular biochemical cascade that begins with the activation of the mGluR7 receptor, it is important to consider whether the experimental facts so far obtained permit of an alternative conclusion.

One such alternative might begin with the fact that direct stimulation of the parallel fibers triggers antidromic volleys of action potentials, as well as orthodromic volleys. Might these antidromic signals reach the Purkinje cell by a path other than the directly stimulated parallel fibers? Several colleagues, reviewers and speakers at scholarly meetings have suggested this as an alternative explanation. We consider this possibility with reference to the diagram of cerebellar circuitry in **Figure 20**.

Antidromic volleys in parallel fibers could excite Golgi cells, which are inhibitory interneurons. However, Golgi cells inhibit the granule cells, which are the source of the parallel fibers. They do not inhibit the Purkinje cells, so this antidromic pathway would appear to be a dead end so far as explaining the conditional pause. We know of no other way that an antidromic signal in a population of directly stimulated parallel fibers could reach a population of unstimulated parallel fibers (see **Figure 20**). Thus, the hypothesis that there are unstimulated granule cells excited by antidromic signals in the stimulated parallel fibers requires the postulation of an unknown pathway and the postulation of the requisite grandmother-cell dynamics for the unstimulated granule-cells. There is neither evidence nor independent motivation for either postulate.

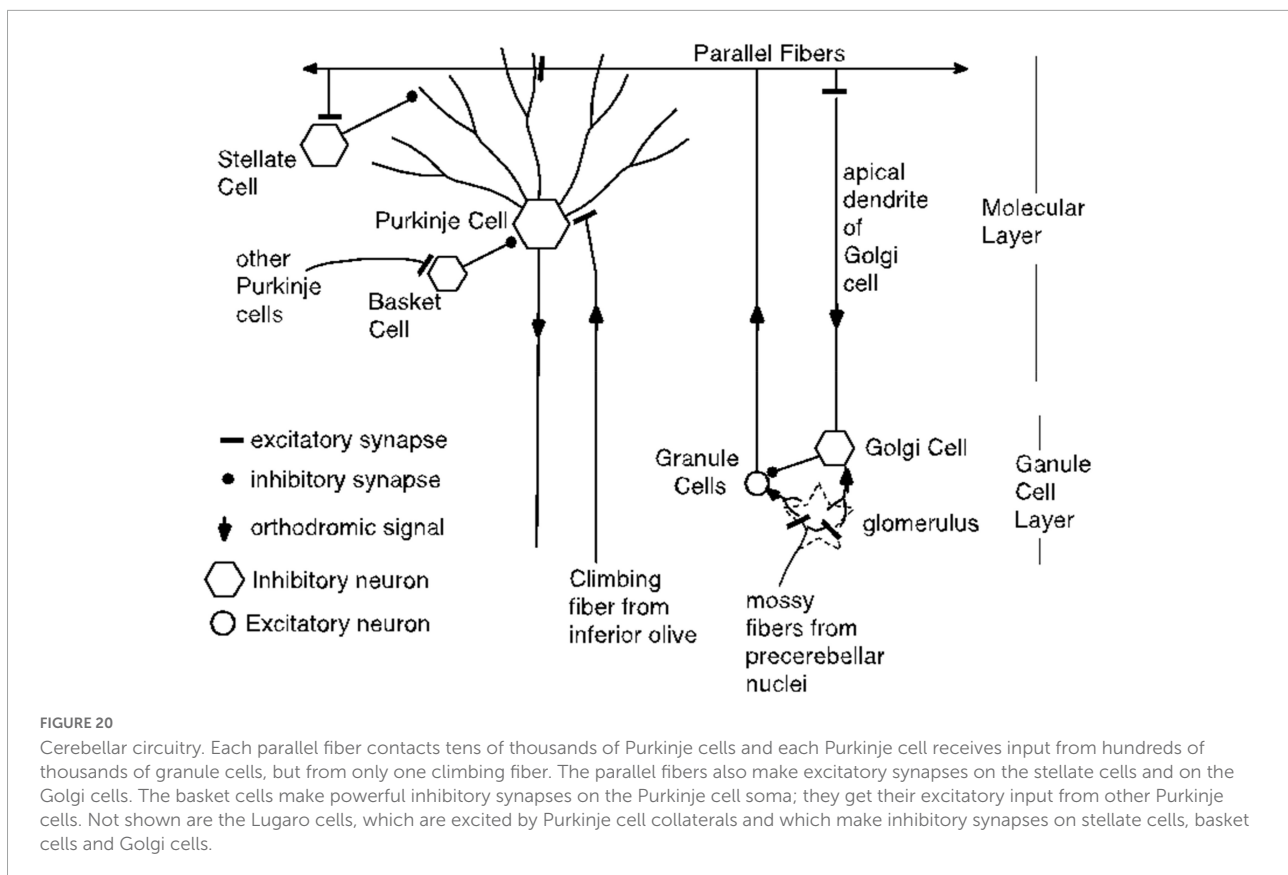
Parallel fibers also excite stellate cells, which make inhibitory (GABAergic) synapses on the outer reaches of Purkinje cell dendrites. (This effect need not be considered antidromic). However, potentiation of the parallel-fiber-to-stellate cell synapse cannot mediate the conditional pause, because the climbing fiber does not innervate the stellate cell. That is, the stellate cell does not have access to both the CS and the US signals. This access is essential to the conditioning of an appropriately timed pause. Instead their inputs consist of far fewer parallel fibers and excitation from multiple climbing fibers only through diffusion of spillover glutamate from climbing fibers that contact Purkinje cells (Szapiro and Barbour, 2007). This is directly opposite to the Purkinje cell whose input architecture enables more than 100,000 different parallel fiber inputs to predict one and only one climbing fiber input.

One might, however, entertain the following hypothesis: Parallel fiber stimulation excites a population of inhibitory stellate cells (antidromically, orthodromically or both). The excited population consists of temporal grandmother cells with an appropriate range of delayed-peak response latencies. The climbing fiber stimulation selectively and enduringly enhances the postsynaptic effects of the GABA released onto the Purkinje cell from those stellate grandmother cells whose firing peaks at the time of climbing fiber stimulation. This inhibitory action of GABA is not blocked by doses of gabazine sufficient to block the profound inhibitory effect of off-beam stimulation.

The following considerations weigh against this alternative hypothesis:

- It does not explain why blocking the mGluR7 receptor blocks the conditional pause. The mGluR7 receptor is postsynaptic to the glutamatergic parallel fiber input to the Purkinje cell. It is not postsynaptic to the stellate cell GABAergic input, nor is it a GABA receptor. Thus, on this hypothesis, there appears to be no explanation for the fact that blocking the mGluR7 receptor blocks the conditional pause; whereas blocking any of the other 7 post-synaptic receptor types in the glutaminergic synapse does not.
- There is no evidence that the stellate cells have the requisite dynamics.
- A fortiori, there is no evidence that these dynamics are triggered by the first volley in parallel fiber and are unaffected by the temporal distribution of subsequent volleys. Known synaptic mechanisms rarely have the latter property.
- There is no evidence that gabazine, a general-purpose GABA blocker, fails to block the inhibitory effect of the GABA that the stellate cells release onto the Purkinje cells. It is the preferred blocker of GABA action.

In the light of current neuroanatomical, neuropharmacological and electrophysiological evidence, there does not appear to be a plausible alternative to the



hypothesis that the mechanisms that time, record and read out the CS-US interval in eyeblink conditioning are intrinsic to the cerebellar Purkinje cell.

Implications of the current results for the putative intracellular engram-reading processes

- The pause is created by an abrupt shut down of the mechanism that generates the rapid but extremely irregular spontaneous firing of the Purkinje cell. The pause is not a graded modulation of that endogenous firing rate; it is a complete shutdown, with no measurable sloping off in the firing rate prior to the cessation of firing.
- The shutdown is triggered by the arrival of the first synchronic volley of nerve impulses in a subset of directly stimulated presynaptic parallel fibers.
- Later volleys have no effect on the pause, regardless of their temporal distribution. If there is no cell-intrinsic temporal memory, there has to be a temporal code in the input signal. It seems impossible to reconcile that assumption with the fact that the elicited pause is the same whether stimulation of the parallel fibers lasts 20 ms or several hundred milliseconds and whether the pulse frequency is 50 Hz or 500 Hz.
- When the CS-US interval is short, the latency to shut down of the firing can be shorter than 20 ms; the engram read-out mechanism can shut down firing in less than 20 ms after the synaptic input that triggers read-out.
- The pause onset latency is, however, determined by the engram for the duration of the CS-US interval, because the latency to shut down firing is proportional to the duration of that remembered interval.
- The latency to terminate the shutdown is also determined by the duration engram; it, too, is proportional to the duration of the remembered interval.
- The correlation structure for the pause parameters implies that the two latencies are produced by independent readings of the engram: The offset (\downarrow) and onset (\uparrow) of the shutdown are only weakly and inconsistently correlated (see the $\downarrow v \uparrow$ correlations in **Figures 16, 19**). This stochastic independence has the consequence that the duration of the shutdown (M) is strongly negatively correlated with onset latency ($M v \uparrow$ in **Figures 16, 19**) and strong positively correlated with offset latency ($\uparrow v \downarrow$ in **Figures 16, 19**, scatterplots). In other words, a late onset of the pause predicts a short shutdown and an early offset retrodicts a short shutdown. If both latencies were determined by a single reading of the duration engram, these latter correlations would have positive sign.

- The process leading to the initiation of the shutdown and the process leading to its termination are independently initiated by the synaptic input that causes the reading of the engram. If the process leading to termination were initiated by the onset of the shutdown, then the latency to terminate the shutdown would be positively correlated with the latency to initiate it and the CoV of the shutdown latency would be greater than the CoV of the initiation latency. In fact, however, the two latencies are uncorrelated or even weakly and inconsistently negatively correlated (Figures 16, 19), and the CoV of the termination latency is smaller than the CoV of the onset latency (Figure 18, compare bottom middle panel to bottom left panel).
- The endogenous spike-generating process is not Poisson. The Fano Factors are generally much greater than expected from a stationary Poisson process. The distribution of the endogenously generated interspike intervals has an extremely abrupt rise after a “refractory” interval that ranges from 3 to 8 ms, depending on the cell. The steep rise is followed by an initially steep decline and then by a remarkably prolonged tail. The tail includes the very long interspike intervals that constitute the conditional pauses. However, when these occur at any time other than immediately after CS onset, their duration is not proportional to the CS-US interval, the interval encoded in the engram.
- The greatly prolonged tail in the inter-spike interval distribution of the spontaneously firing Purkinje cell means that pauses like those that constitute the conditional pause appear often. Whatever the process is that produces these spontaneous pauses, the process that produces the CS-conditional pause can preempt or supervene on a spontaneous pause. The unusually long interspike intervals that constitute the conditional pause (most often a single such interval) may begin during one of the spontaneously occurring long interspike intervals. When the CS-US interval is short, this often produces a conditional pause that appears to begin before CS onset.

A molecular biological agenda

The engram is the mechanism that preserves facts gleaned from experience for use in computations to be performed in the indefinite future. The simplest and most readily varied facts are the quantitative facts. The duration of the interval between two events, such as the onset of a conditional stimulus and the event that it predicts, is an example of an easily varied quantitative fact. The encoded duration of the CS-US interval, plays two fundamental roles in associative learning (Gibbon and Balsam, 1981; Gallistel and Gibbon, 2000; Balsam et al.,

2002, 2006, 2010; Drew et al., 2005; Balsam and Gallistel, 2009; Ward et al., 2012; Gallistel and Balsam, 2014; Morè and Jensen, 2014):

- The duration of the CS-US interval and whether that duration is fixed or variable determines the latency at which the conditional response follows the onset of the CS, and, the pattern of responding within the CS.
- The ratio between the average CS-US interval and the average US-US interval determines the learning rate (trials to acquisition) and the vigor of responding during the CS.

Because the Purkinje-cell engram preserves the duration of the CS-US interval that the cell has experienced, there must be an invertible (one-one) mapping between the duration of an experienced interval and the structural change it produces in the engram. In other words, there must be a code (Gallistel, 2017). Because the engram appears to be intrinsic to the Purkinje cell, one may infer that the structural change that encodes the duration of the CS-US interval is a change in a cell-intrinsic, molecular-level structure. Thus, a key step in the discovery of the material realization of the engram must be the deciphering of the code that relates a molecular change within the Purkinje cell to the duration of the inter-event interval that induces it and that it encodes. The discovery of such a mapping would be powerful evidence that the material realization of the engram (or at least an engram) had at long last been discovered. Decisive evidence would come from artificially inducing the structural modification that encoded a given interval and demonstrating that the duration of the firing pause in response to parallel-fiber input is predicted by that modification. This confirmation of the cell-intrinsic molecular-engram hypothesis would be analogous to the eventual confirmation of two hypotheses that were once profoundly controversial: (1) brains contain clocks (Richter, 1922; Beiling, 1929; Wahl, 1932); (2) the clock is a molecular-level cell-intrinsic mechanism that does not depend on neural circuitry for its function (Bruce and Pittendrigh, 1957; Ralph et al., 1990; Le Sauter and Silver, 1994; Silver et al., 1996). Neuroscientists have been slow to recognize the role of molecular level cell-intrinsic mechanisms in the complex computations that are the foundation of cognition.

The search for the molecular engram in the Purkinje cell should probably begin with a focus on the metabotropic mGlu7 receptor, because blocking that receptor prevents presynaptic input from the parallel fibers from triggering the conditional pause. Metabotropic receptors convert extracellular signals (the transmitter release by a presynaptic spike) into intracellular

biochemical cascades. The first step in most such cascades is a structural change in a G protein. G-protein-initiated cascades are known to lead to alterations in many aspects of cellular physiology, including gene transcription. In this case, the cascade must read the engram before it comes to the membrane-intrinsic ionic channel or channels whose modification abruptly shuts down endogenous firing, because the latency to the shutting down of the endogenous firing is determined by the encoded duration. Given this knowledge and the further facts revealed by this analysis, it seems that a concerted investigation of this intracellular biochemical cascade might bear fruit within a reasonable time span.

Data availability statement

The raw data and the code that analyzed them are available in this publicly accessible repository (<https://github.com/CRGallistel/QuantPropPrkjPauseGH>).

Ethics statement

The animal study was reviewed and approved by Malmö-Lund Animal Research Ethics Committee.

Author contributions

CG and MR developed methods and analyzed data. FJ, D-AJ, and AR contributed with data. FJ, D-AJ, AR, and GH

contributed to results interpretation. CG wrote the initial draft. All authors contributed to manuscript revision, read, and approved the submitted version.

Funding

This work was supported by grants from the Swedish Research Council to GH (2018-03191), to FJ (2019-02034) and to AR (2020-01468), from the Åke Wiberg Foundation, the Magnus Bergvall Foundation and Swedish Brain Foundation to FJ, from Åke-Wiberg Foundation (M19-0375) to AR, and by NSF Graduate Research Fellowship, Award no. 1644760 to MR.

Conflict of interest

The authors declare that the research was conducted in the absence of any commercial or financial relationships that could be construed as a potential conflict of interest.

Publisher's note

All claims expressed in this article are solely those of the authors and do not necessarily represent those of their affiliated organizations, or those of the publisher, the editors and the reviewers. Any product that may be evaluated in this article, or claim that may be made by its manufacturer, is not guaranteed or endorsed by the publisher.

References

- Apps, R., and Garwicz, M. (2005). Anatomical and physiological foundations of cerebellar information processing. *Nat. Rev. Neurosci.* 6, 297–311. doi: 10.1038/nrn1646
- Arcediano, F., and Miller, R. R. (2002). Some constraints for models of timing: A temporal coding hypothesis perspective. *Learn. Motiv.* 33, 105–123. doi: 10.1006/lmot.2001.1102
- Balsam, P. D., Drew, M. R., and Gallistel, C. R. (2010). Time and associative learning. *Comp. Cogn. Behav. Rev.* 5, 1–22. doi: 10.3819/ccbr.2010.50001
- Balsam, P. D., Drew, M. R., and Yang, C. (2002). Timing at the start of associative learning. *Learn. Motiv.* 33, 141–155. doi: 10.1006/lmot.2001.1104
- Balsam, P. D., Fairhurst, S., and Gallistel, C. R. (2006). Pavlovian contingencies and temporal information. *J. Exp. Psychol. Anim. Behav. Process.* 32, 284–294. doi: 10.1037/0097-7403.32.3.284
- Balsam, P. D., and Gallistel, C. R. (2009). Temporal maps and informativeness in associative learning. *Trends Neurosci.* 32, 73–78. doi: 10.1016/j.tins.2008.10.004
- Bareš, M., Apps, R., Avanzino, L., Breska, A., D'Angelo, E., Filip, P., et al. (2018). Consensus paper: Decoding the contributions of the cerebellum as a time machine. From neurons to clinical applications. *Cerebellum* 18, 266–286. doi: 10.1007/s12311-018-0979-5
- Barnet, R. C., Cole, R. P., and Miller, R. R. (1997). Temporal integration in second-order conditioning and sensory preconditioning. *Anim. Learn. Behav.* 25, 221–233. doi: 10.3758/BF03199061
- Bernstein, J. (1871). *Untersuchungen über den Erregungsvorgang in Nerven- und Muskelsysteme*. Heidelberg: Winter.
- Beiling, I. (1929). Über das zeitgedächtnis der bienen. *Zeitschr. Vergl. Physiol.* 9, 259–338.
- Bruce, V. G., and Pittendrigh, C. S. (1957). Endogenous rhythms in insects and microorganisms. *Am. Nat.* 91, 179–195.
- Buonomano, D. V. (2017). *Your brain is a time machine: The neuroscience and physics of time*. New York, NY: W.W. Norton.
- Chandran, M., and Thorwart, A. (2021). Time in associative learning: A review on temporal maps. *Front. Hum. Neurosci.* 15:617943. doi: 10.3389/fnhum.2021.617943
- D'Angelo, E., Solinas, S., Mapelli, J., Gandolfi, D., Mapelli, L., and Prestori, F. (2013). The cerebellar Golgi cell and spatiotemporal organization of granular layer activity. *Front. Neural Circuits* 7:93. doi: 10.3389/fncir.2013.00093
- Denniston, J. C., Blaisdell, A. P., and Miller, R. R. (1998). Temporal coding affects transfer of serial and simultaneous inhibitors. *Anim. Learn. Behav.* 26, 336–350. doi: 10.3758/BF03199226
- Drew, M. R., Zupan, B., Cooke, A., Couvillon, P. A., and Balsam, P. D. (2005). Temporal control of conditioned responding in goldfish. *J. Exp. Psychol. Anim. Behav. Process.* 31, 31–39. doi: 10.1037/0097-7403.31.1.31
- Du Bois-Reymond, E. (1848). *Untersuchungen über thierische Elektrizität*. Berlin: Reimer. doi: 10.1515/9783111475325

- Eden, U. T., and Kramer, M. A. (2010). Drawing inferences from Fano factor calculations. *J. Neurosci. Methods* 190, 149–152. doi: 10.1016/j.jneumeth.2010.04.012
- Freeman, J. H. (2015). Cerebellar learning mechanisms. *Brain Res.* 1621, 260–269. doi: 10.1016/j.brainres.2014.09.062
- Gallistel, C. R. (2017). The coding question. *Trends Cogn. Sci.* 21, 498–508. doi: 10.1016/j.tics.2017.04.012
- Gallistel, C. R. (2021). The physical basis of memory. *Cognition* 213:104533. doi: 10.1016/j.cognition.2020.104533
- Gallistel, C. R., and Balsam, P. D. (2014). Time to rethink the neural mechanisms of learning and memory. *Neurobiol. Learn. Mem.* 108, 136–144. doi: 10.1016/j.nlm.2013.11.019
- Gallistel, C. R., and Gibbon, J. (2000). Time, rate, and conditioning. *Psychol. Rev.* 107, 289–344. doi: 10.1037/0033-295X.107.2.289
- Gallistel, C. R., and Gibbon, J. (2001). Computational versus associative models of simple conditioning. *Curr. Dir. Psychol. Sci.* 10, 146–150.
- Gallistel, C. R., and Matzel, L. D. (2013). The neuroscience of learning: Beyond the Hebbian synapse. *Annu. Rev. Psychol.* 64, 169–200. doi: 10.1146/annurev-psych-113011-143807
- Gallistel, C. R., Balsam, P. D., and Fairhurst, S. (2004). The learning curve: Implications of a quantitative analysis. *Proc. Natl. Acad. Sci. U.S.A.* 101, 13124–13131. doi: 10.1073/pnas.0404965101
- Gallistel, C. R., Shizgal, P., and Yeomans, J. S. (1981). A portrait of the substrate for self-stimulation. *Psychol. Rev.* 88, 228–273. doi: 10.1037/0033-295X.88.3.228
- Gershman, S. J., Moustafa, A. A., and Ludvig, E. A. (2014). Time representation in reinforcement learning models of the basal ganglia. *Front. Comput. Neurosci.* 7:194. doi: 10.3389/fncom.2013.00194
- Gibbon, J. (1977). Scalar expectancy theory and Weber's Law in animal timing. *Psychol. Rev.* 84, 279–335. doi: 10.1037/0033-295X.84.3.279
- Gibbon, J. (1992). Ubiquity of scalar timing with a Poisson clock. *J. Math. Psychol.* 36, 283–293. doi: 10.1016/0022-2496(92)90041-5
- Gibbon, J., and Balsam, P. D. (1981). "Spreading associations in time," in *Autoshaping and conditioning theory*, eds C. M. Locurto, H. S. Terrace, and J. Gibbon (New York, NY: Academic), 219–253.
- Gibbon, J., Church, R. M., and Meck, W. H. (1984). "Scalar timing in memory," in *Timing and time perception*, Vol. 423, eds J. Gibbon and L. Allan (New York, NY: New York Academy of Sciences), 52–77. doi: 10.1111/j.1749-6632.1984.tb23417.x
- Grossberg, S. (1991). "A neural network architecture for Pavlovian conditioning: Reinforcement, attention, forgetting, timing," in *Neural network models of conditioning and action*, eds M. L. Commons, S. Grossberg, and J. E. R. Staddon (Hillsdale, NJ: Lawrence Erlbaum Associates), 69–122.
- Grossberg, S., and Schmajuk, N. A. (1991). "Neural dynamics of adaptive timing and temporal discrimination during associative learning," in *Pattern recognition by self-organizing neural networks*, eds G. A. Carpenter and S. Grossberg (Cambridge, MA: MIT Press), 637–674.
- Hardy, N., and Buonomano, D. V. (2018). Encoding time in feedforward trajectories of a recurrent neural network model. *Neural Comput.* 30, 378–396. doi: 10.1162/neco_a_01041
- Heiney, S. A., Kim, J., Augustine, G. J., and Medina, J. F. (2014). Precise control of movement kinematics by optogenetic inhibition of Purkinje cell activity. *J. Neurosci.* 34, 2321–2330. doi: 10.1523/JNEUROSCI.4547-13.2014
- Helmholtz, H. (1850). Messungen über den zeitlichen Verlauf der Zuckung animalischer Muskeln und die Fortpflanzungsgeschwindigkeit der Reizung in den Nerven. *Arch. Anat. Physiol. Wiss. Med.* 17, 276–364.
- Helmholtz, H. (1852). Messungen über Fortpflanzungsgeschwindigkeit der Reizung in den Nerven. *Arch. Anat. Physiol. Wiss. Med.* 19, 199–216.
- Hesslow, G. (1994a). Correspondence between climbing fibre input and motor output in eyeblink-related areas in cat cerebellar cortex. *J. Physiol.* 476, 229–244. doi: 10.1113/jphysiol.1994.sp020126
- Hesslow, G. (1994b). Inhibition of classically conditioned eyeblink responses by stimulation of the cerebellar cortex in the decerebrate cat. *J. Physiol.* 476, 245–256. doi: 10.1113/jphysiol.1994.sp020127
- Hesslow, G., and Ivarsson, M. (1994). Suppression of cerebellar Purkinje cells during conditioned responses in ferrets. *Neuroreport* 5, 649–652. doi: 10.1097/00001756-199401000-00030
- Hesslow, G., and Yeo, C. H. (2002). "The functional anatomy of skeletal conditioning," in *A neuroscientist's guide to classical conditioning*, ed. J. W. Moore (New York, NY: Springer), 86–146. doi: 10.1007/978-1-4419-8558-3_4
- Honig, W. K. (1981). "Working memory and the temporal map," in *Information processing in animals: Memory mechanisms*, eds N. E. Spear and R. R. Miller (Hillsdale, NJ: Erlbaum), 167–197.
- Jirenhed, D.-A., Bengtsson, F., and Hesslow, G. (2007). Acquisition, extinction, and reacquisition of a cerebellar cortical memory trace. *J. Neurosci.* 27, 2493–2502. doi: 10.1523/JNEUROSCI.4202-06.2007
- Jirenhed, D.-A., and Hesslow, G. (2016). Are Purkinje cell pauses drivers of classically conditioned blink responses? *Cerebellum* 15, 526–534. doi: 10.1007/s12311-015-0722-4
- Jirenhed, D.-A., Rasmussen, A., Johansson, F., and Hesslow, G. (2017). Learned response sequences in cerebellar Purkinje cells. *Proc. Natl. Acad. Sci. U.S.A.* 114, 6127–6132. doi: 10.1073/pnas.1621132114
- Johansson, F. (2015). *A Purkinje cell timing mechanism: On the physical basis of a temporal duration memory*. Ph.D. thesis. Lund: Lund University.
- Johansson, F. (2019). Intrinsic memory of temporal intervals in cerebellar Purkinje cells. *Learn. Mem.* 166:107103. doi: 10.1016/j.nlm.2019.107103
- Johansson, F., Carlsson, H. A. E., Rasmussen, A., Yeo, C. H., and Hesslow, G. (2015). Activation of a temporal memory in Purkinje cells by the mGluR7 receptor. *Cell Rep.* 13, 1741–1746. doi: 10.1016/j.celrep.2015.10.047
- Johansson, F., Hesslow, G., and Medina, J. F. (2016). Mechanisms for motor timing in the cerebellar cortex. *Curr. Opin. Behav. Sci.* 8, 53–59. doi: 10.1016/j.cobeha.2016.01.013
- Johansson, F., Jirenhed, D.-A., Rasmussen, A., Zucc, R., and Hesslow, G. (2014). Memory trace and timing mechanism localized to cerebellar Purkinje cells. *Proc. Natl. Acad. Sci. U.S.A.* 111, 14930–14934. doi: 10.1073/pnas.1415371111
- Kalmbach, A., Chun, E., Taylor, K., Gallistel, C. R., and Balsam, P. D. (2019). Time-scale-invariant information-theoretic contingencies in discrimination learning. *J. Exp. Psychol. Anim. Learn. Cogn.* 45, 280–289. doi: 10.1037/xan0000205
- Kalmbach, A., Winiger, V., Jeong, N., Asok, A., Gallistel, C. R., Balsam, P. D., et al. (2022). Dopamine encodes real-time reward availability and transitions between reward availability states on different timescales. *Nat. Commun.* 13:3805. doi: 10.1038/s41467-022-31377-2
- Kehoe, E., Olsen, K. N., Ludvig, E. A., and Sutton, R. S. (2009). Scalar timing varies with response magnitude in classical conditioning of the nictitating membrane response of the rabbit (*Oryctolagus cuniculus*). *Behav. Neurosci.* 123, 212–217. doi: 10.1037/a0014122
- Kehoe, E. J., Ludvig, E. A., and Sutton, R. S. (2010). Timing in trace conditioning of the nictitating membrane response of the rabbit (*Oryctolagus cuniculus*): Scalar, nonscalar, and adaptive features. *Learn. Mem.* 17, 600–604. doi: 10.1101/lm.1942210
- Kelly, T. M., Zuo, C.-C., and Bloedel, J. R. (1990). Classical conditioning of the eyeblink reflex in the decerebrate-decerebellate rabbit. *Behav. Brain Res.* 38, 7–18. doi: 10.1016/0166-4328(90)90019-B
- Kheifets, A., Freestone, D., and Gallistel, C. R. (2017). Theoretical implications of quantitative properties of interval timing and probability estimation in mouse and rat. *J. Exp. Anal. Behav.* 108, 39–72. doi: 10.1002/jeab.261
- Knierem, J. (1997). "Cerebellum," in *Neuroscience on line: An open-access neuroscience electronic textbook* (Houston, TX: University of Texas Health Sciences Center & McGovern Medical School). Available online at: <https://nba.uth.tmc.edu/neuroscience/s3/chapter05.html> (accessed October 20, 2022).
- Kotani, S., Kawahara, S., and Kirino, Y. (2002). Classical eyeblink conditioning in decerebrate guinea pigs. *Eur. J. Neurosci.* 15, 1267–1270. doi: 10.1046/j.1460-9568.2002.01963.x
- Kritchevsky, M., Squire, L. R., and Zouzonis, J. A. (1988). Transient global amnesia: Characterization of anterograde and retrograde amnesia. *Neurology* 38, 213–219. doi: 10.1212/WNL.38.2.213
- Krupa, D. J., Thompson, J. K., and Thompson, R. F. (1993). Localization of a memory trace in the mammalian brain. *Science* 260, 989–991. doi: 10.1126/science.8493536
- Langille, J. J., and Gallistel, C. R. (2020). The search for the engram: Should we look for plastic synapses or information-storing molecules? *Neurobiol. Learn. Mem.* 169:107164. doi: 10.1016/j.nlm.2020.107164
- Le Sauter, J., and Silver, R. (1994). Suprachiasmatic nucleus lesions abolish and fetal grafts restore circadian gnawing rhythms in hamsters. *Restor. Neurol. Neurosci.* 6, 135–143. doi: 10.3233/RNN-1994-6207
- Li, Y., and Dudman, J. T. (2013). Mice infer probabilistic models for timing. *Proc. Natl. Acad. Sci. U.S.A.* 110, 17154–17159. doi: 10.1073/pnas.1310666110
- Llinas, R. R., Walton, K. D., and Lang, E. J. (2004). "Chapter 7: Cerebellum," in *The synaptic organization of the brain*, ed. G. M. Shepherd (New York, NY: Oxford University Press). doi: 10.1093/acprof:oso/9780195159561.003.0007

- Luce, R. D. (1991). *Response times: Their role in inferring elementary mental organization*. New York, NY: Oxford University Press. doi: 10.1093/acprof:oso/9780195070019.001.0001
- Ludvig, E. A., Sutton, R. S., and Kehoe, E. J. (2008). Stimulus representation and the timing of reward-prediction errors in models of the dopamine system. *Neural Comput.* 20, 3034–3054. doi: 10.1162/neco.2008.11-07-654
- Martin, S. J., and Morris, R. G. M. (2002). New life in an old idea: The synaptic plasticity and memory hypothesis revisited. *Hippocampus* 12, 609–636. doi: 10.1002/hipo.10107
- Mattell, M. S., and Della Valle, R. B. (2018). Temporal specificity in Pavlovian-to-instrumental transfer. *Learn. Mem.* 25, 8–20. doi: 10.1101/lm.046383.117
- Matzel, L. D., Held, F. P., and Miller, R. R. (1988). Information and expression of simultaneous and backward associations: Implications for contiguity theory. *Learn. Motiv.* 19, 317–344. doi: 10.1016/0023-9690(88)90044-6
- Mauk, M. D., and Buonomano, D. V. (2004). The neural basis of temporal processing. *Annu. Rev. Neurosci.* 27, 307–340.
- Mauk, M. D., and Thompson, R. F. (1987). Retention of classically conditioned eyelid responses following acute decerebration. *Brain Res.* 403, 89–95. doi: 10.1016/0006-8993(87)90126-0
- McCormick, D. A., and Thompson, R. F. (1984). Cerebellum: Essential involvement in the classically conditioned eyelid response. *Science* 223, 296–299. doi: 10.1126/science.6701513
- Meck, W. H. (ed.) (2003). *Functional and neural mechanisms of interval timing*. New York, NY: CRC Press. doi: 10.1201/9780203009574
- Medina, J. F., and Ruffolo, L. I. (2014). Cerebellar-dependent expression of motor learning during eyeblink conditioning in head-fixed mice. *J. Neurosci.* 34, 14845–14853. doi: 10.1523/JNEUROSCI.2820-14.2014
- Milner, B., Corkin, S., and Teuber, H. (1968). Further analysis of the hippocampal amnesic syndrome: 14-year follow-up. *Neuropsychologia* 6, 215–234. doi: 10.1016/0028-3932(68)90021-3
- More, L., and Jensen, G. (2014). Acquisition of conditioned responding in a multiple schedule depends on the reinforcement's temporal contingency with each stimulus. *Learn. Mem.* 21, 258–262. doi: 10.1101/lm.034231.113
- Namboodiri, V. M. K., and Stuber, G. D. (2021). The learning of prospective and retrospective cognitive maps within neural circuits. *Neuron* 109, 3552–3575. doi: 10.1016/j.neuron.2021.09.034
- Norman, R. J., Buchwald, J. S., and Villablanca, J. R. (1977). Classical conditioning with auditory discrimination of the eye blink in decerebrate cats. *Science* 196, 551–553. doi: 10.1126/science.850800
- Ohyama, T., and Mauk, M. D. (2001). Latent acquisition of timed responses in cerebellar cortex. *J. Neurosci.* 21, 682–690. doi: 10.1523/JNEUROSCI.21-02-00682.2001
- Papachristos, E. B., and Gallistel, C. R. (2006). Autoshaped head poking in the mouse: A quantitative analysis of the learning curve. *J. Exp. Anal. Behav.* 85, 293–308. doi: 10.1901/jeab.2006.71-05
- Poo, M.-M., Pignatelli, M., Ryan, T. J., Tonegawa, S., Bonhoeffer, T., Martin, K. C., et al. (2016). What is memory? The present state of the engram. *BMC Biol.* 14:40. doi: 10.1186/s12915-016-0261-6
- Ralph, M. R., Foster, R. G., Davis, F. C., and Menaker, M. (1990). Transplanted suprachiasmatic nucleus determines circadian period. *Science* 247, 975–978. doi: 10.1126/science.2305266
- Richter, C. P. (1922). A behavioristic study of the activity of the rate. *Psychol. Monogr.* 1, 1–55.
- Salafia, W. R., Mis, F. W., Terry, W. S., Bartosiak, R. S., and Daston, A. P. (1973). Conditioning of the nictitating membrane response of the rabbit (*Oryctolagus cuniculus*) as a function of length and degree of variation of intertrial interval. *Anim. Learn. Behav.* 1, 109–115. doi: 10.3758/BF03214574
- Savastano, H. I., and Miller, R. R. (1998). Time as content in Pavlovian conditioning. *Behav. Process.* 44, 147–162. doi: 10.1016/S0376-6357(98)00046-1
- Schneiderman, N., and Gormezano, I. (1964). Conditioning of the nictitating membrane of the rabbit as a function of CS-US interval. *J. Comp. Physiol. Psychol.* 57, 188–195. doi: 10.1037/h0043419
- Siebert, R. J., and Warrington, E. K. (1996). Spared retrograde memory with anterograde amnesia and widespread cognitive deficits. *Cortex* 32, 177–185. doi: 10.1016/S0010-9452(96)80026-8
- Silver, R., LeSauter, J., Tresco, P., and Lehman, M. N. (1996). A diffusible coupling signal from the transplanted suprachiasmatic nucleus controlling circadian locomotor rhythms. *Nature* 382, 810–813.
- Simen, P., Rivest, F., Ludvig, E. A., and Killeen, P. (2013). Timescale invariance in the pacemaker-accumulator family of timing models. *Timing Time Percept.* 1, 159–188. doi: 10.1163/22134468-00002018
- Solomon, P. R., Stowe, G. T., and Pendlebury, W. W. (1989). Disrupted eyelid conditioning in a patient with damage to cerebellar afferents. *Behav. Neurosci.* 103, 898–902. doi: 10.1037/0735-7044.103.4.898
- Szapiro, G., and Barbour, B. (2007). Multiple climbing fibers signal to molecular layer interneurons exclusively via glutamate spillover. *Nat. Neurosci.* 10, 735–742. doi: 10.1038/nn1907
- Taylor, K. M., Joseph, V., Zhao, A. S., and Balsam, P. D. (2014). Temporal maps in appetitive Pavlovian conditioning. *Behav. Process.* 101, 15–22. doi: 10.1016/j.beproc.2013.08.015
- Ten Brinke, M. M., Heiney, S. A., Wang, X., Proietti-Onori, M., Boele, H. J., Bakermans, J., et al. (2017). Dynamic modulation of activity in cerebellar nuclei neurons during Pavlovian eyeblink conditioning in mice. *eLife* 6:e28132. doi: 10.7554/eLife.28132
- Thompson, R. F., and Steinmetz, J. E. (2009). The role of the cerebellum in classical conditioning of discrete behavioral responses. *Neurosci.* 162, 732–755. doi: 10.1016/j.neuroscience.2009.01.041
- Wahl, O. (1932). Neue untersuchungen über das zeitgedächtnis der bienen. *Zeitschr. Vergl. Physiol.* 16, 529–589.
- Ward, R. D., Gallistel, C. R., and Balsam, P. D. (2013). It's the information! *Behav. Process.* 95, 3–7. doi: 10.1016/j.beproc.2013.01.005
- Ward, R. D., Gallistel, C. R., Jensen, G., Richards, V. L., Fairhurst, S., and Balsam, P. D. (2012). Conditional stimulus informativeness governs conditioned stimulus-unconditioned stimulus associability. *J. Exp. Psychol. Anim. Behav. Process.* 38, 217–232. doi: 10.1037/a0027621
- White, N. E., Kehoe, E. J., Choi, J.-S., and Moore, J. W. (2000). Coefficients of variation in timing of the classically conditioned eyeblink in rabbits. *Psychobiology* 28, 520–524. doi: 10.3758/BF03332010
- Yamazaki, T., and Tanaka, S. (2009). Computational models of timing mechanisms in the cerebellar granular layer. *Cerebellum* 8, 423–432. doi: 10.1007/s12311-009-0115-7
- Yeo, C. H. (1991). Cerebellum and classical conditioning of motor responses. *Ann. N. Y. Acad. Sci.* 627, 292–304. doi: 10.1111/j.1749-6632.1991.tb25933.x
- Yeo, C. H., Hardiman, M. J., and Glickstein, M. (1984). Discrete lesions of the cerebellar cortex abolish the classically conditioned nictitating membrane response of the rabbit. *Behav. Brain Res.* 13, 261–266. doi: 10.1016/0166-4328(84)90168-2
- Yeo, C. H., Hardiman, M. J., and Glickstein, M. (1985a). Classical conditioning of the nictitating membrane response of the rabbit. I. Lesions of the cerebellar nuclei. *Exp. Brain Res.* 60, 87–98. doi: 10.1007/BF00237022
- Yeo, C. H., Hardiman, M. J., and Glickstein, M. (1985b). Classical conditioning of the nictitating membrane response of the rabbit. II. Lesions of the cerebellar cortex. *Exp. Brain Res.* 60, 99–113. doi: 10.1007/BF00237023
- Yeo, C. H., Hardiman, M. J., and Glickstein, M. (1986). Classical conditioning of the nictitating membrane response of the rabbit. IV. Lesions of the inferior olive. *Exp. Brain Res.* 63, 81–92. doi: 10.1007/BF00235649